



Network Level Study as a Promising Approach in the Brain Mapping

Gholam-Ali Hossein-Zadeh * 

School of Electrical and Computer Engineering, College of Engineering, University of Tehran, Tehran, Iran

*Corresponding Author: Gholam-Ali Hossein-Zadeh
Email: ghassemi@aut.ac.ir

Abstract

Number of publications on the use of network/connectivity analysis in the fundamental and clinical neuroscience are increasing. This creates the promise to understand the link between the brain and behavior by this approach. In this preface to the published extended abstracts of Iranian Symposium Brain Mapping (ISBM) 2022, I point to some methods of network study of the brain and highlight the benefits of the approach.

Keywords: Brain Mapping; Network Analysis; Connectivity; Iranian Symposium Brain Mapping 2022.

1. Different Approaches of Network Study of the Brain

As more years are passing from the development of fMRI and neuroimaging techniques, studies are more concentrated on higher level cognitive processes, and functional integration. It seems that the network approach may help to link the brain and behavior, thus helping to direct the fundamental science to the applied [1]. A central expectation in brain mapping is that how brain network features form the human behavior, and more importantly relates to brain health. As an example Chen *et al.* in [2] showed that network features can predict cognitive performance, personality scores and mental health assessments in a large sample of adolescence neuroimaging data.

Diffusion weighted MRI provides a noninvasive tool to investigate the structural connectivity of the brain. Whereas the structural networks provided by this modality is a key factor in pre-surgical planning, and clinical diagnosis of some brain disorders like stroke, they are also applicable to choose the best stimulation points of a structural network in invasive and non-invasive brain stimulation.

Neuroimaging guided brain stimulation can also benefit from the network point of view by targeting the most effective nodes of an important network that can later affect a behavior, or treat a brain disorder. A good example may be the Stanford neuromodulation therapy. This noninvasive neuroimaging based TMS therapy benefits from the functional connectivity analysis at the individual level to target a specific part of DLPFC which make the intervention very effective.

2. Conclusion and Acknowledgment

The evidences of emerging network/connectivity approaches to study the brain is visible among the speeches, panels and accepted papers in the sixth Iranian symposium of brain mapping updates ISBM 2022. The accepted and presented papers which are published in this especial issue were reviewed by expert reviewers of symposium and were the best among tens of submitted papers. I would like to appreciate the FBT journal for organizing this issue.

References

- 1- Tessa F. Blanken, Joe Bathelt, Marie K. Deserno, Lily Voge, Denny Borsboom, Linda Douw, "Connecting brain and behavior in clinical neuroscience: A network approach.", *Neuroscience & Biobehavioral Reviews*, Volume 130, p. 81-90, (2021).
- 2- Jianzhong Chen, Angela Tam, Valeria Kebets, Csaba Orban, Leon Qi Rong Ooi, Christopher L. Asplund, Scott Marek, Nico U. F. Dosenbach, Simon B. Eickhoff, Danilo Bzdok, Avram J. Holmes & B. T. Thomas Yeo, "Shared and unique brain network features predict cognitive, personality, and mental health scores in the ABCD study.", *Nature Communications*, vol, 13, 2217, (2022).



Emotion Classification from EEG Signals Using Differential Entropy Feature and SVM

Narges Hosseini* , Babak Mohammadzadeh Asl

Department of Electrical and Computers Engineering, Tarbiat Modares University, Tehran, Iran

*Corresponding Author: Narges Hosseini
Email: Nargeshosseini199564@gmail.com

Abstract

Emotion recognition as one of the mental states that has a direct effect on all cognitive behaviors and physical activities of human can help to recognize some of the facts in the human mind. Recently, research on the human nervous system has been performed using Electroencephalography (EEG), which contains the best and most complete emotional information while being complex. In this research an emotion recognition system is developed based on valence/arousal model using EEG signals. These signals are decomposed into theta, alpha, beta and Gamma bands using Discrete Wavelet Transform (DWT), and time domain, frequency domain and time-frequency domain features are extracted from each frequency band. Support Vector Machine (SVM), Probabilistic Neural Network (PNN) and Adaboost are used to classify emotional state. The cross validated SVM with RBF Kernel using differential entropy with recursive Copola division (DEC) performs with 89% accuracy for valence and 91% accuracy for arousal. Our approach shows better performance compared to existing algorithms which using just one feature applied to the "DEAP" dataset.

Keywords: Emotion Recognition; Electroencephalography Signals; Classification; Wavelet Transform; Support Vector Machine.

1. Introduction

Emotions are a manifestation of intuitive states of the mind. As a hot topic in affective computing area, emotion recognition has recently caught more attentions. The responses of emotion can be characterized by behavioral and physiological signals because it is people’s psychophysiological reactions to internal or external stimuli. The EEG signals are suitable tool for current research this signals are generated by the Central Nervous System (CNS) and respond more rapidly to emotional changes than other peripheral neural signals. Moreover, EEG signals have been shown to provide important features for emotional recognition [1].

The EEG signals are generated by electrical waves corresponding to brain activity presented by external stimuli [2]. In the design of an emotion recognition system, selection of effective features and accurate classification are two important steps. from EEG signals, in intelligent emotion recognition systems. The wavelet transform is able to decompose signals in specific frequency bands. To this end, choosing an appropriate mother wavelet is crucial. Murugappan [3] considered four different mother wavelets, namely ‘db4’, ‘db8’, ‘sym8’ and ‘coif5’ to extract the statistical features, including standard deviation, power and entropy from EEG signal. The KNN classifier was employed and the accuracy rate was about 82.87% on 62 channels and 78.57% on 24 channels. Zhang et al. [4] use three methods to select the best channels to classify the four emotions (joy, fear, sadness and relaxation) using SVM classifier, and the best classification accuracy over 19 channels is 59.13% ± 11.00%. In literature, various nonlinear parameters are used to capture the underlying characteristics of the emotions-labeled EEG signals [5]. The H-jorth parameter [6], the fractal and multi-fractal dimension [6,7] and the different variant of differential entropy [5,6] are used to characterize human emotions.

2. Materials and Methods

1. Dataset: In this paper, we used data from the DEAP dataset that have been post-processed in MATLAB. In this dataset, 32 subjects viewed 40 clips of video, and for each video, seven physiological

modalities were recorded: EEG, EMG, Electrooculography (EOG), skin temperature, respiration pattern, blood volume pressure and GSR.

2. Channel selection: Reduce Dimensions, faster processing and improved model performance are important reasons for channel selection. In this paper we apply Anova method for channel selection.

3. Preprocess: In this section, we used the CSSP spatial filter, which is an improved version of CSP method.

4. Feature extraction: The human brain is a typical nonlinear dynamic system, so the nonlinear dynamic features of brain electrical signals reflect emotion information. In this paper Power spectrum density and statistical properties such as median and variance, Fractal dimension, H_jorth parameters, entropy, wavelet energy, wavelet entropy and Differential Entropy with recursive Copola division (DEC) are used. On the 60 seconds data in each channel. It should be noted that the differential entropy with recursive Copola division is a characteristic of a relatively continuous random variable.

DEC:

$$H = - \int_{R^n} p(x) \ln p(x) dx \tag{1}$$

Following the Sclar theorem, any continuous multidimensional density can be written as follows:

$$P(x) = p_1(x_1) \dots p_D(x_D) c(F_1(x_1), \dots, F_D(x_D)) \tag{2}$$

P_k is a cumulative distribution and $c(u_1, \dots, u_D)$ is Pair density.

$$\left[\prod_{j=1, \dots, D, j \neq k} \int du_j \right] c(u_1, \dots, u_D) = 1 \tag{3}$$

$$H = \sum_{k=1}^D H_k + H_c \tag{4}$$

H_k is Marginal entropy of order K and H_c is Pair entropy.

Differential entropy is obtained from the sum of marginal entropy and pair entropy. To get the entropy of the pair:

$$c(u_1, \dots, u_D) = p(F_1(x_1), \dots, F_D(x_D)) \quad (5)$$

In general for each $k=1, \dots, D$, σ_k is Represents permutation of $\{1, \dots, N\}$ and:

$$u_k^i = \frac{1}{N} (\sigma_k^i - \frac{1}{2}) \quad (6)$$

The above expression is called the user interface of duplicate copola, which is divided into two equal parts. These two parts are: $v_j^i = \{u_j^i | u_k^i \leq \frac{1}{2}\}$ and $w_j^i = \{u_j^i | u_k^i \geq \frac{1}{2}\}$. Scale these halves as $2v_j^i$ and $2w_j^i$ Generates two new sample sets for the Copola, so the pair entropy will be as follows:

$$H_c = 1/2(H_{2v} + H_{2w-1}) \quad (7)$$

5. Classification: In this study we applied 3 methods for classification including SVM, PNN and Adaboost.

3. Results

In the DEAP dataset, the length of each trial is equal to 63 seconds, the first 3 seconds correspond to the baseline. For faster and more accurate processing, we also separated the 25 to 35 seconds of the trial, as mentioned in [8], and applied all the processing to these 10 seconds. We implemented 4 approaches to achieve the best result. We first describe the 4 approaches and then compare the 4 approaches in terms of valence and arousal through diagrams.

Approach 1: Use 4 features of variance, median, power spectrum density and fractal dimension.

Approach 2: Apply the above 4 features along with H-jorth parameters, entropy, wavelet entropy, wavelet energy and sample entropy parameters and use Mutual information feature selection.

Approach 3: This approach included the fractal dimension, power spectrum density, and differential entropy.

Approach 4: Use only one feature which was improved differential entropy with recursive copola.

We compare each of these approaches with three different classification models.

As shown in the [Figure 1](#), the 4th approach with the SVM classification has the best results in both directions.

4. Conclusion

In this study, we tried to achieve an efficient emotion recognition system by using the differential entropy feature and different classifiers such as SVM, PNN and Adaboost. We first extracted the 32-user raw EEG signals from the DEAP stand-alone database, and then used the CSSP spatial filter to facilitate the separation of the two classes of data. After applying the spatial filter, we proceeded to extract the features and chose differential entropy from among all the extracted features due to the decrease in processing speed and increased accuracy. Finally, we presented four approaches to classification and found that SVM had higher processing speeds in addition to higher accuracy.

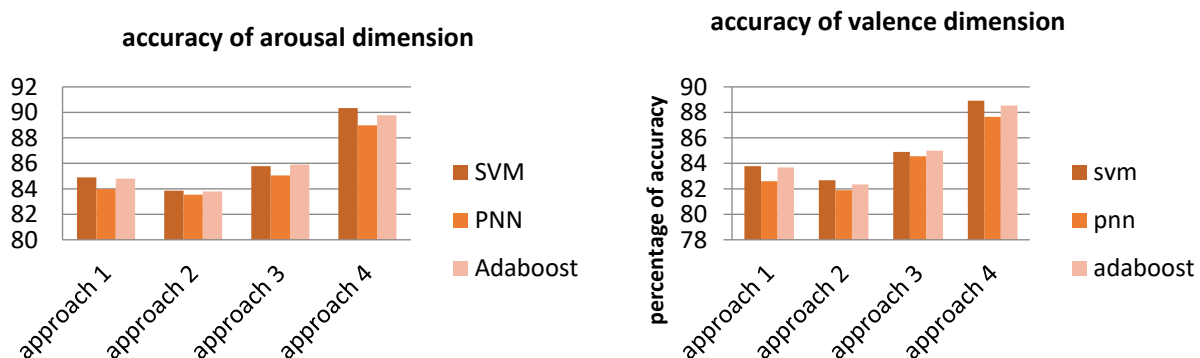


Figure 1. accuracy of valence and arousal dimension for 4 approach

References

- 1- Ansari-Asl, K., G. Chanel, and T. Pun. "A channel selection method for EEG classification in emotion assessment based on synchronization likelihood.", in *2007 15th European Signal Processing Conference, IEEE*, (2007).
- 2- Lubis, N., et al., "Positive emotion elicitation in chat-based dialogue systems.", *IEEE/ACM Transactions on Audio, Speech, and Language Processing*, 27(4): p. 866-877, (2019).
- 3- Murugappan, M. "Human emotion classification using wavelet transform and KNN. in 2011 International Conference on Pattern Analysis and Intelligence Robotics." *IEEE*, (2011).
- 4- Zhang, J., et al., "Relief-based EEG sensor selection methods for emotion recognition.", *Sensors*, 16(10): p. 1558, (2016).
- 5- Zheng, W.-L. and B.-L. Lu, "Investigating critical frequency bands and channels for EEG-based emotion recognition with deep neural networks.", *IEEE Transactions on Autonomous Mental Development*, 7(3): p. 162-175, (2015).
- 6- Thammasan, N., et al., "Continuous music-emotion recognition based on electroencephalogram.", *IEICE TRANSACTIONS on Information and Systems*, 99(4): p. 1234-1241, (2016).
- 7- Zheng, W.-L., J.-Y. Zhu, and B.-L. Lu, "Identifying stable patterns over time for emotion recognition from EEG.", *IEEE Transactions on Affective Computing*, 10(3): p. 417-429, (2017).
- 8- Petrantonakis, P.C. and L.J. Hadjileontiadis, "A novel emotion elicitation index using frontal brain asymmetry for enhanced EEG-based emotion recognition.", *IEEE Transactions on information technology in biomedicine*, 15(5): p. 737-746, (2011).



Real-Time EEG-Based Person Identification Using Convolutional Neural Network

Mahdi Mohammadi* , Ali Nouri

Department of Biomedical Engineering, Amirkabir University of Technology, Tehran, Iran

*Corresponding Author: Mahdi Mohammadi

Email: Mahdi.mohammadi@aut.ac.ir

Abstract

Biometric authentication, or the use of physical characteristics to identify people, has become more common in recent years and is used in many of our everyday devices, like smartphones and wearable devices. The Electroencephalogram (EEG) can also be used for this purpose as a non-invasive and relatively low-cost method. High security, reliance on the user's mental state, and compatibility with widely used brain-computer interface systems are among the advantages of this technique, which motivated this research. In this study, a convolutional neural network is used to demonstrate the effectiveness of brain electrical signals in identifying people, and several aspects of the performance of such systems are investigated. The proposed neural network recognizes 109 people with 95.42% accuracy using a one-second epoch of EEG signals from the EEGMMI dataset recorded in 64 channels. The accuracy of the proposed model with 32 and 16 channels is 92.18% and 90.02%, respectively. By comparing the performance of different frequency bands, it is shown that the gamma frequency band has the highest accuracy and the delta band has the lowest in biometric applications.

Keywords: Biometrics; Electroencephalogram; Convolutional Neural Network; Classification.

1. Introduction

Identity recognition has traditionally been done by passwords or smart cards. However, these methods have a number of drawbacks, including the risk of forgetting, theft, or loss. Biometrics are relatively newer methods of identification that use biological or behavioral characteristics of individuals such as fingerprints, faces, voices, gaits, and Electroencephalography (EEG). With the development of inexpensive brainwave recording devices, the use of EEG signals for biometrics has attracted the attention of researchers. This biometer has the advantage of being very difficult to counterfeit or steal, as well as having an association with the user's memory, mood, and mental state, which makes it unique [1]. Despite the growing popularity of EEG biometrics, most studies have relied on manual feature extraction methods, and relatively few studies have applied deep learning or used raw temporal signals. According to these studies, and considering that EEG signals have both spatial and temporal properties, convolutional neural networks appear to be an excellent choice for extracting features and classification [1].

2. Materials and Methods

The data used in this study is from Physionet's public EEG Motor Movement/Imagery Dataset (EEGMMIDB) [2]. The signals are collected from 109 subjects with a sampling rate of 160 Hz using 64 electrodes arranged in accordance with the international 10-10 system specifications. For each subject, there are 14 experimental trials: two baseline runs conducted in resting-state conditions (one with eyes open and the other with eyes closed) and twelve runs including opening and closing fists and feet (six imaginary movement tasks and six physical ones).

Before feeding the data to the neural network, a pre-processing procedure has been done in three steps. First, the frequency bands of the brain signal were separated using Finite Impulse Response (FIR) filters. Next, each recording of data is normalized by scaling so that the data's minimum and maximum values are zero and one, respectively. Then, all of the recordings are segmented into one-second epochs with no overlap. This brings the total number of records from

1,500 to around 170,000 epochs of 1-second data and 1,560 per subject. Each data epoch is a 64×160 matrix containing 160 samples recorded in a second with 64 channels.

A convolutional neural network is proposed to classify EEG signals in this study, which consists of four convolutional, four max pooling, and a fully-connected layer. After each convolutional layer, a max pooling layer is utilized, followed by a fully-connected layer. The number of convolutional layers' filters is 128, 256, 512, and 1024, with each filter having a 2×2 dimension. The same padding is used in these layers, and therefore the dimensions of the input and output matrices are equal. So, the max pooling layers with 2×2 filters and the stride of 2 are responsible for reducing the dimension of the input data. These layers lower the complexity and computational cost by reducing the parameters, as well as the possibility of over-fitting. A dropout with a rate of 0.5 is also considered to reduce the probability of overfitting in the fully connected layer. Finally, Adam optimization method with a learning rate of 0.01 is utilized in this network.

3. Results

Three groups of tests were performed to evaluate the proposed method. First, the model's overall performance was assessed using data from 12 task records, namely trials 3 through 14. In this assessment, after mixing the order of these records, 9 trials for training data and 3 trials for test data were randomly selected. This process was repeated four times according to the 4-fold cross-validation approach, and the average accuracy was 95.421% with a variance of 0.684. In another analysis, the neural network performance was compared across different frequency bands. For each subject, four recordings were used, including trials 1 through 4. As the results of these experiments are shown in Table 1, in all four trials, the gamma band has the highest accuracy in identification, the beta band comes in second, and the delta band comes in last.

Evaluating the effects of user mode resulted in a 97.05% accuracy with the data from trial 1 (open eyes) and a 94.30% accuracy in trial 2 (closed eyes). Additionally, comparisons of the rest mode (combination of trials 1 and 2) and task mode

(combination of trials 3 and 4) showed 96.46% and 96.75% accuracy, respectively. Finally, with 32 and 16 channels, the network performed with 92.18% and 90.20% accuracy, respectively.

Table 1. Accuracy of the network for each frequency band for four trials

Trial Number	1	2	3	4	Average	Variance
Frequency Band	Accuracy (%)					
Delta	56.82	59.70	60.09	50.85	56.86	13.65
Theta	66.25	68.61	61.60	57.86	63.58	17.26
Alpha	67.43	65.01	61.47	61.34	63.81	6.53
Beta	89.19	84.80	83.94	88.04	86.50	4.78
Gamma	97.97	97.44	97.51	96.53	97.36	0.27
Full band	97.05	94.30	96.13	96.00	95.87	0.98

4. Conclusion

The proposed method is able to recognize 109 people using a one-second epoch of EEG signal with 95.421% accuracy. The best performance, according to some prior studies [3, 4], was in the gamma frequency range. There was no significant difference in performance between the resting state and data from motor or visual tasks. However, in the closed-eye recording mode, a slight decrease in accuracy was observed.

References

- 1- Bidgoly, Amir, Hamed Jalaly Bidgoly, and Zeynab Arezoumand. "A survey on methods and challenges in EEG based authentication.", *Computers & Security*, 93 (2020).
- 2- Goldberger, A., et al. "PhysioBank, PhysioToolkit, and PhysioNet: Components of a new research resource for complex physiologic signals.", *Circulation* [Online]. 101 (23), pp. e215–e220, (2000).
- 3- Wang, M., H. El-Fiqi, J. Hu, and H. A. Abbass. "Convolutional neural networks using dynamic functional connectivity for EEG-based person identification in diverse human states.", *IEEE Transactions on Information Forensics and Security*, 14, no. 12 (2019).
- 4- Boubakeur, Meriem R., and Guoyin Wang. "Self-Relative Evaluation Framework for EEG-Based Biometric Systems.", *Sensors*, 21, no. 6 (2021).



Investigation of Task Engagement Index in Mobile BCI Systems Based on Steady-State Visually Evoked Potentials

Amin Abdipourasl* , Zahra Tabanfar, Ali Nouri

Department of Biomedical Engineering, Amirkabir University of Technology, Tehran, Iran

*Corresponding Author: Amin Abdipourasl
Email: abdipoursepehr@gmail.com

Abstract

Steady-State Visually Evoked Potentials (SSVEPs), a response to flickering visual stimuli, are a popular paradigm in BCI systems. BCI tasks typically necessitate a high cognitive workload as well as a long working duration, which can result in decreased vigilance, errors, and task failure. This issue is exacerbated in mobile BCI since the user must move in the surroundings in addition to focusing on the task. The task engagement index (TEI) is a ratio of EEG power bands ($\beta/(\alpha + \theta)$) that can be used to determine the user's cognitive engagement in a specified task. When the user's mental engagement with the relevant task is reduced, this index can be used as a warning system. In this research, TEI was calculated for 23 healthy participants while they were standing, slow walking, fast walking, and slightly running at speeds of 0, 0.8, 1.6, and 2.0 m/s, respectively. Moreover, the accuracy of target frequency detection was calculated using the traditional CCA method. The results show that the trend change of TEI at different speeds is consistent with the accuracy obtained by the CCA method. Based on this, it can be concluded that increasing the speed of movement reduces the user's mental engagement with the relevant task, which may affect the performance of target stimulus frequency detection systems.

Keywords: Brain-Computer Interface; Task Engagement Index; Steady-State Visually Evoked Potentials; Canonical Correlation Analysis.

1. Introduction

Noninvasive EEG-based BCI systems have received a lot of attention in the previous decade due to their ease of use, low cost, and superior temporal resolution. EEG paradigms such as Motor Imagery (MI), Event-Related Potentials (ERPs), and Steady-State Visually Evoked Potentials (SSVEPs) are commonly used in EEG-based BCI systems. In the SSVEP paradigm, Visual stimuli are used to trigger activity in the brain's visual cortex. The frequency of evoked activity is usually the same as the frequency of the flickering visual stimuli. Therefore, in the analysis of these signals, the occipital regions of the brain (visual cortex) are often taken into account [1]. The effortful attentiveness and striving towards task goals has been termed as engagement. Pope *et al.* [2] developed the first brain-based adaptive system that relied on an EEG-based task engagement measures. The system made use of a bio-cybernetic loop, which was formed by adjusting the level of automation in response to changes in cognitive workload demands. They found that the engagement index based on the ratio $\beta/(\alpha + \theta)$ was shown to be the most sensitive of the potential indices they examined. Further research by Freeman *et al.* [3] validated the $\beta/(\alpha + \theta)$ index's effectiveness. When the engagement index was used to motivate adjustments in the stimulus presentation, they reported better performance in a vigilance task. In this study, TEI is calculated for EEG signal in different channels. These EEG signals are acquired in a mobile BCI environment. As a result, the effect of speed on user engagement can be investigated. Finally, the accuracy of user command identification is calculated using CCA and the relationship between TEI and system performance (based on accuracy criteria) will be measured.

2. Materials and Methods

To evaluate the proposed methodology, we use an online available mobile SSVEP dataset [4] collected at different speeds. The dataset contains 32 channels (based on 10-20 international system) of EEG signals acquired from 23 healthy individuals while looking at three stimulus frequencies (5.45, 8.57, and 12 Hz) for 5 seconds displayed at the left, center, and right of an LCD monitor. Participants walked on a treadmill at different speeds of 0, 0.8, 1.6, and 2.0 m/s (only 16 participants did the 2.0 m/s test). Finally, the performance of the TE index in measuring the user's mental engagement was evaluated by comparing the trend of alteration in this criterion with the trend of alteration in the accuracy of target stimulus frequency recognition obtained by the CCA method.

3. Results

Figure 1 depicts the calculated TEI values for 2 channels of Oz (due to its proximity to the visual cortex) and F4 (based on [5]) and four speeds (for each participant). As can be seen, the highest TEI was obtained in the first session when participants did not move (speed 0 m/s) and the lowest TEI was obtained in the fourth session when participants moved with the fastest speed. Based on this, it can be concluded that as speed increases, the user's attention to the task decreases. Figure 2 depicts the average TEI value for each session for all participants. This Figure also includes the accuracy rate of target frequency detection based on the CCA approach for each speed to help evaluate the strategy.

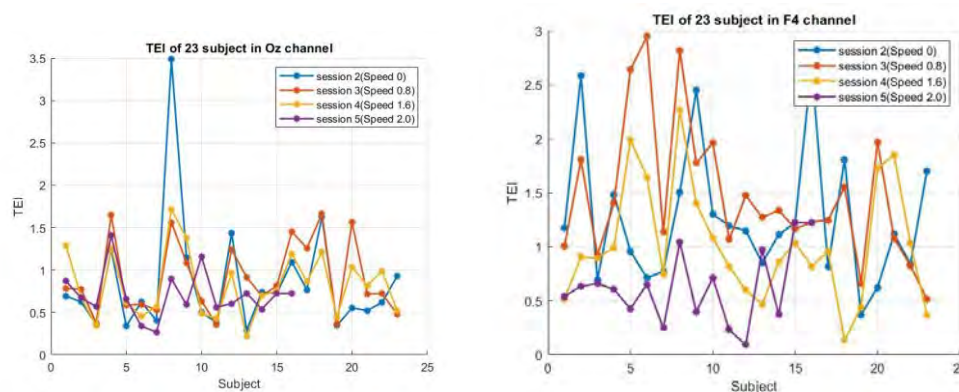


Figure 1. TEI value for 23 Participants in (a) Oz and (b) F4 channels

As illustrated in Figure 2, the average TEI values follows the same pattern as the accuracy rate obtained using the CCA method. It may be stated that as the user's attention to the work rises, so does their speed.

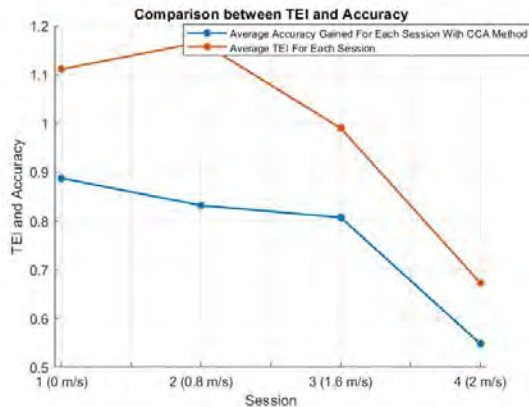


Figure 2. Comparison of the average TEI value of 23 subjects and the accuracy calculated using the CCA method

4. Conclusion

Based on the findings, it can be concluded that TEI can be used in SSVEP-based BCI systems to provide a user distraction alert system. However, some modifications to this criterion are required, such as user-based normalization, which can be investigated in future research.

References

- 1- Ali Nouri and Kyanoosh Azizi, "Introducing a Convolutional Neural Network and Visualization of its Filters for Classification of EEG Signal for SSVEP Task." *Frontiers in Biomedical Technologies*, Vol. 7 (No. 3), pp. 151-58, (2020).
- 2- Alan T Pope, Edward H Bogart, and Debbie S Bartolome, "Biocybernetic system evaluates indices of operator engagement in automated task." *Biological psychology*, Vol. 40 (No. 1-2), pp. 187-95, (1995).
- 3- Frederick G Freeman, Peter J Mikulka, Lawrence J Prinzel, and Mark W Scerbo, "Evaluation of an adaptive automation system using three EEG indices with a visual tracking task." *Biological psychology*, Vol. 50 (No. 1), pp. 61-76, (1999).
- 4- Young-Eun Lee, Gi-Hwan Shin, Minji Lee, and Seong-Whan Lee, "Mobile BCI dataset of scalp-and ear-EEGs with ERP and SSVEP paradigms while standing, walking, and running." *Scientific Data*, Vol. 8 (No. 1), pp. 1-12, (2021).

5- Konrad Biercewicz, Mariusz Borawski, and Jarosław Duda, "Method for Selecting an Engagement Index for a Specific Type of Game Using Cognitive Neuroscience." *International Journal of Computer Games Technology*, Vol. 2020, (2020).



The Role of Cognitive Style in Moral Judgment

Negar Karimi^{1,2,3*} , Javad Hatami⁴

¹ Institute for Cognitive and Brain Sciences, Shahid Beheshti University, Tehran, Iran

² Sleep Disorders Research Center, Health Institute, Kermanshah University of Medical Sciences, Kermanshah, Iran

³ Cognitive Science Research Group, Academic Center for Education, Culture and Research, Alborz Branch, Alborz, Iran

⁴ Department of Psychology, Faculty of Psychology and Educational Sciences, University of Tehran, Tehran, Iran

*Corresponding Author: Negar Karimi

Email: Karimi.negarr@gmail.com

Abstract

Many moral controversies involve a tension between individual rights and the greater good. According to the dual-process theory of moral judgment, this is because moral judgments are not produced by a unified “moral faculty. Deontological judgments favoring the rights of the individual are preferentially supported by automatic emotional responses, while utilitarian judgments favoring the greater good are preferentially supported by controlled cognitive processes. The dual-process framework answered some questions but did not clarify what triggers this automatic emotional response. In this study, we began to fill this critical gap and hypothesized that 1) visual imagery preferentially supports deontological moral judgments, and 2) that verbal processing preferentially supports utilitarian moral judgments. 106 participants first performed a working memory task which involved 4 conditions, 2 congruent conditions, and 2 incongruent conditions. According to accuracy and speed of response, the relative cognitive style of visual or verbal was determined. Then they answered 7 high conflict moral dilemmas. The results showed that in incongruent conditions, individuals with relatively visual cognitive style made more deontological judgments (disapproving of sacrificing one person to save the others). In congruent conditions, this relationship did not reach the level of statistical significance. Findings of the relationship between reaction time and moral judgment showed that in incongruent conditions, a higher level of reaction time in visual cognitive style had a significant positive relationship with deontological moral judgment. These findings did not reach the level of statistical significance in congruent conditions.

Keywords: Moral Judgment; Cognitive Style; Visual Imagery; Working Memory.

1. Introduction

Recent research in moral psychology has examined the pervasive tension between the rights of the individual and the greater good, employing moral dilemmas that capture this tension [1-4]. For example, in the classic footbridge dilemma (Thomson, 1985), one can save five lives by pushing an innocent person into the path of a runaway trolley. Research on such dilemmas supports a dual-process theory of moral judgment according to which deontological judgments favoring the rights of the individual (e.g., “It’s wrong to push the man”) are preferentially supported by automatic emotional responses, whereas utilitarian, or consequentialist, judgments favoring the greater good (e.g., “It’s better to save the five”) are preferentially supported by controlled cognition [1,2,5].

As you can see, what dual-process theory emphasizes is the role of the cognitive and emotional neural correlates of moral judgment. In the next step, this theory examines the factors that activate two different systems in the brain.

Studies indicate that visual representations, as compared with verbal representations, are more emotionally salient [6-9]. On the other hand, there is a convergence between the theory of dual-process and the construal level theory [10]. in the field of moral judgment predictions. According to the theory of structural levels, the mental representation of a single object or event is possible at different levels. High-level representations are relatively more abstract and address general goals, while low-level representations are objective, contextual, and instrumental. In low-level representation, when one imagines a purposeful act, the means used to achieve the goal are also represented in the mind. Therefore, when a violent act is a tool to achieve the desired goal, by emphasizing the role of the traumatic tool and objectifying the violent act as much as possible in the mind, it increases the negative emotion in the person and therefore intuitive processing that leads to conscientious judgment. Abstract representation usually manifests itself in the form of language. Verbal representations involve higher levels of abstraction than visual representations. These representations emphasize goals more than means. Thus, in situations where a violent act (for example, sacrificing a person) is the

way to save more lives, emphasizing the result and considering the positive consequences of doing an act, prevents the increase of negative emotion and consequential judgments. Strengthen [11]. As you can see, what the two theories of dual processing and levels of structure emphasize is the role of mental representation of information in the pattern of moral judgments. Caruso and Gino (2011) first examined the role of mental imagery by closing their eyes when making moral judgments and stated that mental imagery highlights the role of all moral considerations [12]. Then Amit and Green (2012) examined the role of mental imagery on the pattern of moral judgments in three experiments with the help of cognitive styles, visual-verbal interference and also questions about the tendency of people to depict harmful tools. The results in all three experiments confirmed the role of mental imagery on the pattern of moral judgments [13].

Considering the importance of mental representations in the field of ethics, the present study investigates the effect of cognitive (visual-verbal) styles on the pattern of moral judgments. It is predicted that visual cognitive style will reduce consequential judgments due to the increase of mental imagery and verbal cognitive style will increase consequential judgments by increasing the amount of abstraction.

2. Materials and Methods

2.1. Participants

106 participants (49 women, 57 men; age range =19–39 years; all native Persian speakers) were recruited. Participants were seated at a computer running Matlab (Version 2010; psych toolbox) software. First, they completed a similarity judgment task. This behavioral task is the same as used in Kraemer, Rosenberg, & Thompson-Schill, 2009 [14] which we first translated into Persian language. As shown in Figure 1, each item in this task consisted of either an image (e.g., a red triangle with stripes) or a set of 3 words that named a shape, color, and pattern (e.g. red, stripes, triangle). In each experimental trial, participants first viewed a target item (either picture or words) in the center of the screen for 1500 ms. Subsequently, two probe items (either two pictures or two sets of words) appeared and remained on screen until the participant responded. There was no time

limit. As targets and probes could be presented either as images or as words, there were four within-subject trial conditions: two congruent conditions (picture-picture, and word-word) and two incongruent conditions (picture word, and word-picture). Participants completed 24 trials of each of these four conditions. Next, participants responded to seven high-conflict personal moral dilemmas in which killing a single person would save several others. The specific personal dilemmas used were Crying Baby, Sophie's Choice, Lifeboat, Safari, Plane Crash, Sacrifice, and Footbridge. Also, three impersonal dilemmas (Fumes, Trolley, and Donation) were included to reduce repetition. Participants judged the moral acceptability of the proposed utilitarian action in each dilemma using a 7-point scale ranging from 1 (completely not appropriate) to 7 (completely appropriate). Dilemmas were randomly ordered in questionnaire. Finally, participants were asked about their gender, age, and number of years of education.

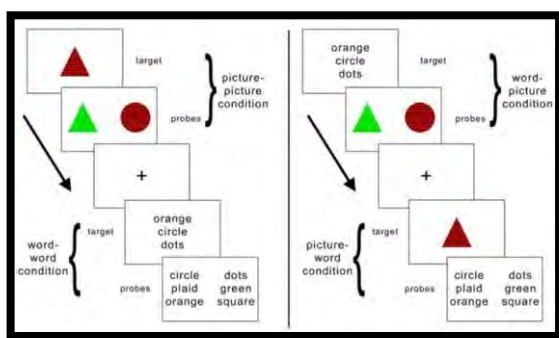


Figure 1. Schematic illustration of task conditions. The similarity judgment requires memory and comparison of a target item to two subsequently presented probe items. On half of the trials the target item is presented as a picture and on the other half it is presented as a set of words that name equivalent features. Likewise, the probes are presented as words on half of the trials and as pictures on the other half

3. Results

For each participant, we computed a Visualizer-Verbalizer (VV) score by subtracting mean verbal accuracy from mean visual accuracy in congruent conditions and also incongruent conditions. Thus, higher numbers indicate a more visual cognitive style. Then, for each participant, we computed the mean moral-acceptability rating for the seven high-conflict

dilemmas. Higher mean ratings indicate more utilitarian judgments, and lower mean ratings indicate more deontological judgments. In congruent conditions (picture-picture vs. word-word), there was no significant correlation between VV score and mean moral-acceptability rating $r(104) = 0.04$, $P\text{-Value} = 0.676$, but in incongruent conditions (picture-word vs. word-picture) there was a significant correlation between VV score and mean moral-acceptability rating, $r(104) = -0.197$, $P\text{-Value} = 0.042$, such that individuals with more visual cognitive styles made judgments that were, on average, more deontological and less utilitarian, favoring the rights of the individual over the greater good. This effect held when we controlled for level of education ($r = -0.197$, $P\text{-Value} = 0.044$), and gender ($r = -0.195$, $P\text{-Value} = 0.046$).

Among 4 conditions, there was a significant correlation between (word-picture) condition and moral judgment, $r(104)$ ($P\text{-Value} = 0.001$, $r = -0.30$), such that individuals with more correct answers in this condition, made judgments that were, on average, more deontological and less utilitarian. There was no significant correlation between word correct answers to three other conditions (picture-picture, word-word and picture-word) and moral judgment. There was also no significant correlation between the reaction time of four conditions and moral judgment.

4. Conclusion

According to these findings, visual imagery has a specific role in moral judgments. When people consider sacrificing someone as a means to an end, visual imagery preferentially supports the judgment that the ends do not justify the means. These results suggest an integration of the dual-process theory of moral judgment with construal-level theory.

References

- 1- Ciaramelli E, Muccioli M, Ladavas E, di Pellegrino G. "Selective deficit in personal moral judgment following damage to ventromedial prefrontal cortex.", *Social Cognitive and Affective Neuroscience*; 2(2):84-92, (2007).
- 2- Cushman F, Young L, Hauser M. "The role of conscious reasoning and intuition in moral judgment: testing three principles of harm.", *Psychological Science*; 17(12):1082-1089, (2006).

- 3- Greene JD, Morelli SA, Lowenberg K, Nystrom LE, Cohen JD. "Cognitive load selectively interferes with utilitarian moral judgment." *Cognition*; 1;107(3):1144-54, (2008).
- 4- Greene JD, Nystrom LE, Engell AD, Darley JM, Cohen JD. "The neural bases of cognitive conflict and control in moral judgment.", *Neuron*; 44(2):389-400, (2004).
- 5- Paxton, J. M., Ungar, L., Greene, J. D. "Reflection and reasoning in moral judgment.", *Cognitive Science*, 35, 1–15, (2011).
- 6- De Houwer, J., Hermans, D. "Differences in the affective processing of words and pictures.", *Cognition & Emotion*, 8, 1–20, (1994).
- 7- Holmes, E. A., Mathews, A. "Mental imagery and emotion: A special relationship?", *Emotion*, 5, 489–497, (2005).
- 8- Holmes, E. A., Mathews, A., Mackintosh, B., Dalgleish, T. "The causal effect of mental imagery on emotion assessed using picture-word cues.", *Emotion*, 8, 395–409, (2008).
- 9- Kensinger, E. A., Schacter, D. L. "Processing emotional pictures and words: Effects of valence and arousal." *Cognitive, Affective, & Behavioral Neuroscience*; 6, 110–126, (2006).
- 10- Trope, Y., Liberman, N. "Construal level theory of psychological distance.", *Psychological Review*, 117, 440–463, (2010).
- 11- Gong, H & Medin, L, D. "Construal levels and moral judgment: Some complication.", *Judgment and Decision Making*; (7) 5. 628-638, (2012).
- 12- Caruso, E. M., Gino, F. "Blind ethics: Closing one's eyes polarizes moral judgments and discourages dishonest behavior.", *Cognition*, 118, 280–285, (2011).
- 13- Amit, E., & Green, J. "You See, the Ends Don't Justify the Means: Visual Imagery and Moral Judgment.", *Psychological Science*, 23, 861-868, (2012).
- 14- Kraemer, D., J. M. Rosenberg., I. M. & Thompson-Schill, S. L. "The neural correlates of visual and verbal cognitive style." *Journal of Neuroscience*, 29 (12). 3792-3798, (2009).



Altered Effective Connectivity in the Default Mode Network between Healthy Control and Autism Patient Groups: A Resting-State fMRI Study

Fatemeh Mansouri¹, Fabrice Wallois², Mahdi Saadatmand^{1*} 

¹Rayan Center for Neuroscience and Behavior & Medical Imaging Lab, Department of Electrical Engineering, Faculty of Engineering, Ferdowsi University of Mashhad, Mashhad, Iran

²INSERM, U1105, GRAMFC, Université de Picardie, CHU Nord, Amiens F80000, France

*Corresponding Author: Mahdi Saadatmand
Email: saadatmand@um.ac.ir

Abstract

Autism Spectrum Disorder (ASD) is a developmental disorder whose cause has not been determined yet. The current study examined 154 participants (77 ASD, 77 Controls, between 5 and 9 years) from nine independent datasets of the ABIDE. Previous studies have often examined functional connectivity, lacking information about the directed causal influences among the brain regions; however, in the present study, we examined the Effective Connectivity (EC) of the Default Mode Network (DMN). Effective connectivity is a measurable parameter of brain network connectivity that infers the causality and directionality of connections between a set of Regions Of Interest (ROIs).

We used Dynamic Causal Modeling (DCM) to DMN with fully model connected, and used the Parameter Empirical Bayes model (PEB) with considered age, gender, handedness, and IQ of each participant for our group analysis.

We found a reduction in effective connectivity the default mode network of autistic patients compared to healthy controls. Reduced effective connectivity from MPFC to RIPC, reduced effective connectivity from PCC to MPFC and reduced effective connectivity from PCC to LIPC. We also found decrease self-inhibition in MPFC and RIPC, and an increase in effective connectivity in the DMN of male with ASD.

Keywords: Effective Connectivity; Autism Spectrum Disorder; Dynamic Causal Modelling; Parameter Empirical Bayes Model; Resting State functional Magnetic Resonance Imaging; Default Mode Network.

1. Introduction

Autism Spectrum Disorder (ASD) is a range of neurodevelopmental situations with significant social communication, and rigid repetitive behaviors [1]. Autism can cause a wide variety of structural and functional changes in the brain. Although many researchers attempted to evaluate structural changes of autistic brains [2], due to the limited communication abilities of these patients, performing task-based functional Magnetic Resonance Imaging (fMRI) is impractical in most cases [3]. Therefore, resting-state fMRI (rs-fMRI) can be considered as the best modality to study brain spontaneous fluctuations and information exchange in brain networks [4].

Generally, based on the rs-fMRI data, the Functional Connectivity (FC) between different nodes of a pre-specified brain network can be assessed by statistical dependency analysis of the corresponding time series. On the other hand, the Default-Mode Network (DMN) plays the most important role in the resting state conditions (see Figure 1). Therefore, in most works performed until now, for studying functional brain changes due to Autism, researchers considered DMN and its variants as the basis network [5]. For example, Reiter *et al.* [6] researched on FC children of 44 ASD patients and 44 controls. The ASD patients were in two groups of lower-functioning and higher-functioning. The findings provided that lower- and higher-functioning ASDs had atypical connectivity that mainly reduced FC in DMN. In another study, Baron-Cohen *et al.* [7] proposed reduced FC in DMN by using Seed-based and group ICA methods on 15 ASD patients and 20 healthy controls. Two further networks (salience and medial temporal lobe) identified by ICA have reduced FC within and between them. Ypma *et al.* [8] studied on a group of 112 autistic patients to evaluation of sex-related differences in DMN. The study revealed that there is significant underconnectivity in DMN which is related to sex-phenotype in extreme case of ASD. Also Floris *et al.* [9] to understand the role of biological sex-related factors in autism used a large sample of male and female children with autism and control (autism: 362 males, 82 females; control: 409 males, 166 females). The result represented a significant main effects of sex differences in functional connectivity of the Posterior Cingulate

Cortex (PCC). Moratal *et al.* [10] researched on 2 groups of ASD patients and controls in 3 categories of children, adolescents and adults. The participants were similar in age and IQ score in each category. The results represented hypoconnectivity in children and adolescents with ASD in DMN region as a reduced FC between the left middle temporal gyrus and right frontal pole, and between the left orbitofrontal cortex and right superior frontal gyrus. Any significant differences were not observed in the adult group. Calvo *et al.* [11] proposed that as age increases in ASD adolescents, connectivity in the dorsal and ventral default mode network become more anterior and posterior, respectively, while in the executive control network, connectivity increases within frontoparietal regions. Lei *et al.* [12] studied effective connectivity (EC) within the social brain network of children with ASD and controls. The data were analyzed with the multivariate Granger causality method. The results represented attenuated effective connectivity from the medial Prefrontal Cortex (mPFC) to the bilateral amygdala in children with the ASD group compared with control group; the amygdala helps with social cognition. Zhou *et al.* [13] evaluated EC of children with autism and healthy control. The EC was measured between 94 brain areas. In autism, the middle temporal gyrus and other temporal areas had lower effective connectivities to the precuneus and cuneus, and the hippocampus and amygdala had higher EC to the middle temporal gyrus. Chen *et al.* [14] proposed evaluation of EC between the thalamus and the cortex in children with autism patients and healthy controls; the results provided reduced EC of thalamotemporal in ASD which was correlated with intensity of communication deficits. Linke *et al.* [15] researched on FC of 24 young children with ASD and 23 typically developing children (aged 17–45 months), Increased Intrinsic functional connectivity between visual and sensorimotor networks was found in young children with ASD compared to control participants. Within the ASD group, the degree of overconnectivity between visual and sensorimotor networks was associated with more significant autism symptoms.

However, functional connectivity can be more effectively studied, if the directional (causal) effect of different nodes is also considered in the network [16].

2. Materials and Methods

We examined 77 healthy controls (TD, mean age 7, male and female) and 77 patients with an autism spectrum disorder (ASD, mean age 7, male and female). All corresponding T1 images and functional images were downloaded from the ABIDE dataset (http://fcon_1000.projects.nitrc.org/indi/abide/). The ABIDE dataset is an open-access multi-site image repository comprising structural and rs-fMRI scans from ASD and TD individuals. Data was acquired from 9 datasets from the ABIDE source. Inclusion criteria for databases were to have, (1) Similar repetition time (TR= 2 ms), (2) children with age between 5-9 years, (3) subjects with information of full IQ, handedness, gender, (4) Children with autism (were not imported the Aspergers and PDD-NOS), and (5) We participated in an equal number of autism and control participants in each age range. We included participants with gender, age, full IQ, and handedness as important covariates. Inclusion as a participant in the ASD group required receiving an ASD diagnosis based on the autism diagnostic observation schedule-generic (ADOS-G) and an expert clinical opinion upon DSM-IV criteria.

2.1. Preprocessing

First, we set the origin of all T1 images (anatomical images) of each participant; the origin is where the intersection of the Anterior (AC), Posterior Commissure (PC), or their midpoint. This point is called “functional coordinates”. When we preprocess fMRI data, we are cleaning up the noise or all fluctuations that we are not interested in. All data were preprocessed using the SPM12 toolbox (<https://www.fil.ion.ucl.ac.uk/spm/software/spm12/>). The steps were as follows. (1) The first step of fMRI preprocessing is to realign the functional images to eliminate head motion artifacts; we registered images to mean images. (2) fMRI volumes are acquired in slices, and the timing of capturing of each slice is different from the other slices, so we use slice timing to correct the difference in timing between slices. (3) To make sure that each voxel for each subject belongs to the same part of the brain, we registered the functional images of each person on their anatomical image, like to the rigid-body transformation with zooms and shears. (4) To remove extra tissue from the

anatomical image, we segmented it. (5) the most essential part of preprocessing is normalization. There are the difference between the shape and size of brains of people, so we need a standard space for fMRI data analysis; we registered the data to MNI125. (6) The last step is smoothing; for spatial filtering, we applied the Gaussian kernel of FWHM = 6*6*6 mm.

2.2. First Level Analysis with DCM

First we need to set up the General Linear Model (GLM) analysis and extract our time series from the results. In this model, our goal is to extract the gray-matter (GM) time series. This model uses one or more regressors (independent variables) to predict an outcome measure (dependent variable). So we specified and estimated the GLM model by adding the White-Matter (WM) and Cerebrospinal Fluid (CSF) time series as regressors and then extracting the time series of the default network from the GLM model that we specified. The default mode network time series is extracted with four important nodes, Medial Prefrontal Cortex (MPFC), Posterior Cingulate Cortex (PCC) and bilateral intraparietal cortex (LIPC, RIPC). We extracted the time series of these four nodes using the volume of interest method (ROIs); [Figure 1a](#) shows the time series of each of these nodes. We built the DCM with time series of each region. DCM partitions the variability in a subject’s time series into neural and non-neural (i.e., hemodynamic and noise) sources that are shown in the [Equation 1](#); this model uses a Taylor approximation to capture the effective connectivity among brain regions and the change in effective connectivity due to experimental inputs [\[17\]](#). We selected the bilinear model to model neural activities and specified the DCM with the fully connected model; in this model all connections should be ‘switched on’, as shown in [Figure 1c](#). The bilinear model captures the change in neural activity per unit time, the [Equation 1](#) says that neural response \dot{Z} depends on connectivity matrix J . The columns of matrix J are the outgoing connections, and the rows are the incoming connections; Parameter matrix C is the sensitivity of each region to driving inputs [\[17\]](#).

$$\dot{Z} = JZ + Cu(t) \quad (1)$$

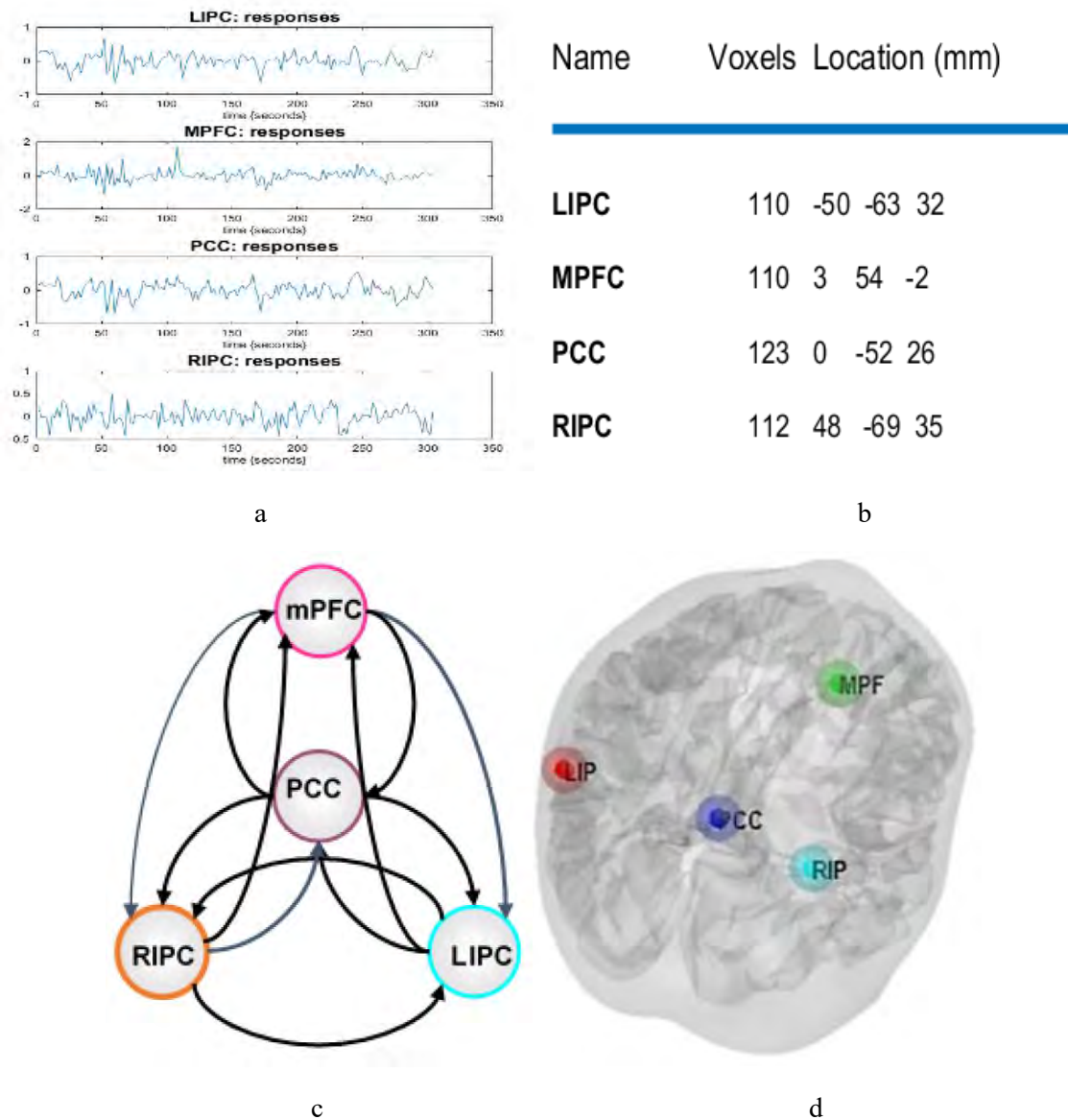


Figure 1. (a) Illustration of the Default Mode Network (DMN) time series, (b) The MNI coordinate of each region, (c) DMN with fully connected model, (d) Location of DMN region

2.3. Second Level Analysis

We specified each subject's DCM for the default mode network, then specified the GDCM (group DCM), and estimated with the Bayesian model, only one DCM is specified per subject, and the estimated parameters are taken to the group level.

2.4. Specifying Parameter Empirical Bayes Model

The PEB framework specifies a hierarchical statistical model of connectivity parameters; this model can add covariate a design matrix to variation across subjects. Each

of these parameters is the group-level effect of one covariate (e.g., LI, handedness, or gender) on one connection [18]. PEB determines the hypotheses about between-subject effects and within-subject effects. We considered age, gender, FIQ, and handedness as the covariates in the PEB model and estimated them with cross-spectral density. Figure 2 shows the group-level parameters (PEB parameters) estimated prior probability.

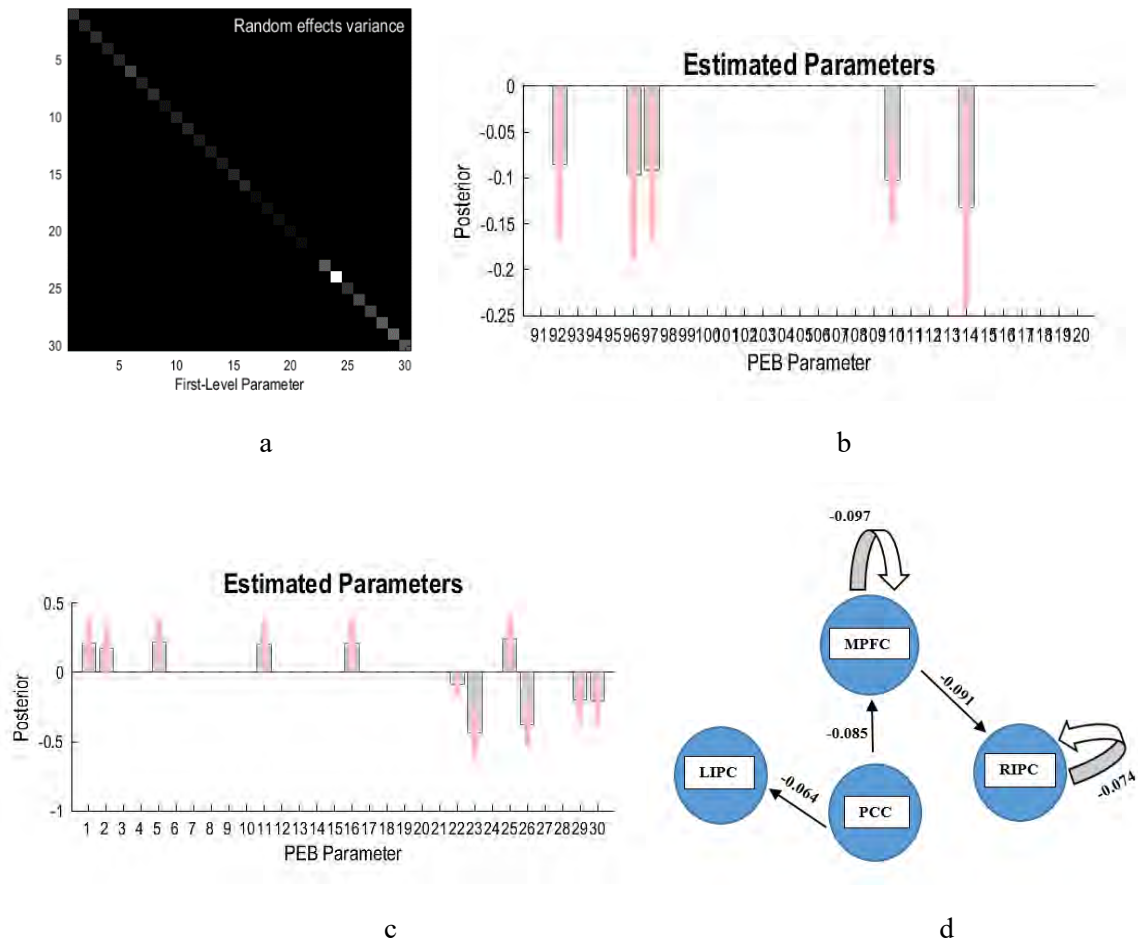


Figure 2. (a) The estimated between-subject covariance matrix (b) The second level effect between ASD and control with the probability of 95% and, (c) the second level effect between ASD and control with the probability of 95% and considering age, gender, IQ and handedness for each subject, and (d) Effective connectivity in DMN of ASD

3. Results

We first identified important regions of the DMN from an independent component analysis and used them as regions of interest for DCM.

We studied effective connectivity among DMN regions, [Figure 2a](#) showed the estimated between-subject covariance matrix for each parameter, where the more white they are, the greater the between-subject variability. The between-group differences in effective connectivity were obtained using the PEB model; the unit of PEB parameters is in hertz. It was found that EC was reduced in the DMN of autistic patients compared to healthy controls ([Figure 2b](#)). Reduce EC from medial prefrontal cortex to right intraparietal cortex ($EC=-0.091\text{Hz}$, probability=0.97), this is in the stronger direction, reduced EC from posterior cingulate cortex to medial prefrontal cortex ($EC=-0.085\text{Hz}$, probability=0.96) and reduced EC

from posterior cingulate cortex to left intraparietal cortex ($EC=-0.064$, probability=0.91). Thus, the pattern for the posterior cingulate cortex in autism is decreased EC to the medial prefrontal cortex and left intraparietal cortex. We also found decreased self-inhibition in the medial prefrontal cortex ($EC=-0.097$, probability=0.96) and right intraparietal cortex ($EC=-0.074$, probability=0.93).

In the study of gender covariate, significant positive EC (or increase EC) were observed from the left intraparietal cortex to: right intraparietal cortex ($EC=0.0115$, probability=0.98), medial prefrontal cortex ($EC=0.068$, probability=0.91), and posterior cingulate cortex ($EC=0.075$, probability=0.94) in the male with autism. Also found significant negative EC (or decrease EC) from right intraparietal cortex to posterior cingulate cortex ($EC=-0.068$, probability=0.93) in the male with autism. So ECs are correlated with gender in this range of age. ECs of

medial prefrontal cortex and bilateral intraparietal cortex increased with age, in the other words these nodes have a riding role in age covariates. In the study of handedness and FIQ covariates, we observed changing the EC parameters of the areas with a gentle slope changed and there were weaker direction in alternation of EC in IQ and handedness; for example in IQ covariate increased EC only 0.002Hz from posterior cingulate cortex to left intraparietal cortex or increased self-inhibition of left intraparietal cortex just 0.002Hz. Therefore, these covariates were not useful in this age range we studied, and ECs changes were not related to IQ and handedness.

4. Conclusion

In this research, we employed DCM to study effective connectivity differences between autism patients and healthy controls in resting-state fMRI. The results indicated evidence of underconnectivity in the default mode network of autism patients, and effective connectivity in autism revealed increased alterations in the male from LIPC to the other regions. Finally, we concluded that studying effective connectivity leads to a better understanding of ASD research.


References

- 1- C. E. Robertson and S. Baron-Cohen, "Sensory perception in autism," *Nature Reviews Neuroscience*, vol. 18, no. 11, pp. 671–684, (2017), doi: 10.1038/nrn.2017.112.
- 2- J. S. Anderson, "Comprehensive Guide to Autism," *Compr. Guid. to Autism*, (2014), doi: 10.1007/978-1-4614-4788-7.
- 3- S. J. Gotts, M. Ramot, K. Jasmin, and A. Martin, "Altered resting-state dynamics in autism spectrum disorder: Causal to the social impairment?," *Prog. Neuro-Psychopharmacology Biol. Psychiatry*, vol. 90, pp. 28–36, (2019), doi: 10.1016/J.PNPBP.2018.11.002.
- 4- S. M. Smith *et al.*, "Functional connectomics from resting-state fMRI," *Trends in Cognitive Sciences*, vol. 17, no. 12, pp. 666–682, (2013), doi: 10.1016/j.tics.2013.09.016.
- 5- M. van den Heuvel, R. Mandl, and H. Hulshoff Pol, "Normalized Cut Group Clustering of Resting-State fMRI Data," *PLoS One*, vol. 3, no. 4, p. e2001, (2008), doi: 10.1371/journal.pone.0002001.
- 6- M. A. Reiter, L. E. Mash, A. C. Linke, C. H. Fong, I. Fishman, and R. A. Müller, "Distinct Patterns of Atypical Functional Connectivity in Lower-Functioning Autism," *Biol. Psychiatry Cogn. Neurosci. Neuroimaging*, (2019), doi: 10.1016/j.bpsc.2018.08.009.
- 7- E. A. H. von dem Hagen, R. S. Stoyanova, S. Baron-Cohen, and A. J. Calder, "Reduced functional connectivity within and between 'social' resting state networks in autism spectrum conditions," *Soc. Cogn. Affect. Neurosci.*, (2013), doi: 10.1093/scan/nss053.
- 8- Y. Gao *et al.*, "The language network in autism: Atypical functional connectivity with default mode and visual regions," *Autism Res.*, vol. 12, no. 9, pp. 1344–1355, (2019), doi: 10.1002/aur.2171.
- 9- D. L. Floris *et al.*, "Towards robust and replicable sex differences in the intrinsic brain function of autism," *Mol. Autism*, vol. 12, no. 1, pp. 1–17, (2021), doi: 10.1186/s13229-021-00415-z.
- 10- L. Borràs-Ferris, Ú. Pérez-Ramírez, and D. Moratal, "Link-level functional connectivity neuroalterations in autism spectrum disorder: A developmental resting-state fMRI study," *Diagnostics*, vol. 9, no. 1, (2019), doi: 10.3390/diagnostics9010032.
- 11- C. Solé-Padullés *et al.*, "Intrinsic connectivity networks from childhood to late adolescence: Effects of age and sex," *Dev. Cogn. Neurosci.*, vol. 17, pp. 35–44, (2016), doi: 10.1016/j.dcn.2015.11.004.
- 12- L. Li *et al.*, "Attenuated link between the medial prefrontal cortex and the amygdala in children with autism spectrum disorder: Evidence from effective connectivity within the 'social brain,'" *Prog. Neuro-Psychopharmacology Biol. Psychiatry*, vol. 111, p. 110147, (2021), doi: 10.1016/J.PNPBP.2020.110147.
- 13- E. T. Rolls, Y. Zhou, W. Cheng, M. Gilson, G. Deco, and J. Feng, "Effective connectivity in autism," *Autism Res.*, vol. 13, no. 1, pp. 32–44, (2020), doi: 10.1002/aur.2235.
- 14- H. Chen, L. Q. Uddin, Y. Zhang, X. Duan, and H. Chen, "Atypical effective connectivity of thalamo-cortical circuits in autism spectrum disorder," *Autism Res.*, vol. 9, no. 11, pp. 1183–1190, (2016), doi: 10.1002/aur.1614.
- 15- B. Chen *et al.*, "Greater functional connectivity between sensory networks is related to symptom severity in toddlers with autism spectrum disorder," *J. Child Psychol. Psychiatry.*, vol. 62, no. 2, pp. 160–170, (2021), doi: 10.1111/JCPP.13268.
- 16- O. Sporns, "The human connectome: A complex network," *Annals of the New York Academy of Sciences*, vol. 1224, no. 1, pp. 109–125, (2011), doi: 10.1111/j.1749-6632.2010.05888.x.

- 17- P. Zeidman *et al.*, “A guide to group effective connectivity analysis, part 1: First level analysis with DCM for fMRI,” *Neuroimage*, vol. 200, pp. 174–190, (2019), doi: 10.1016/j.neuroimage.2019.06.031.
- 18- P. Zeidman *et al.*, “A guide to group effective connectivity analysis, part 2: Second level analysis with PEB,” *Neuroimage*, vol. 200, no. March, pp. 12–25, (2019), doi: 10.1016/j.neuroimage.2019.06.032.



Representation of Confidence in Prediction of Other's Risky Decision Making: An fMRI Study

Ahmad Shoaah Haghighi^{1,2*} , Soroush Safari^{3,4}, Elahe Oloumi^{3,4}, Hadis Jameei², Gholam Ali Hossein Zadeh^{1,4}, Abdol-Hossein Vahabie^{2,3}

¹ School of Electrical and Computer Engineering, University of Tehran, Tehran, Iran

² Control and Intelligent Processing Center of Excellence, Cognitive Systems Laboratory, School of Electrical and Computer Engineering, College of Engineering, University of Tehran, Tehran, Iran.

³ Department of Psychology, Faculty of Psychology and Education, University of Tehran, Tehran, Iran

⁴ School of Cognitive Sciences, Institute for Research in Fundamental Sciences, Tehran, Iran

*Corresponding Author: Ahmad Shoaah Haghighi

Email: a.shoaahaghighi@gmail.com

Abstract

Reporting the confidence after a decision-making task is widely used on the studies of metacognition, a cognitive factor usually defined as “thinking about thinking.” When people predict others’ behavior in risky situations, they consider various factors affecting the others’ choices; at that point, they can determine how confident they are about their predictions about the other’s decision. This study investigates human neural activities in different confidence levels when participants predict others’ financial choices in a risky decision-making task. For this aim, functional Magnetic Resonance Imaging (fMRI) combined with behavioral tasks is used to demonstrate the neural representation of human confidence level about others’ possible choices. The results indicate that the Frontal Pole Cortex (FPC), cingulate gyrus, and precuneus cortex activities are correlated with the confidence of people in their predictions. These key findings suggest that the brain's activities can represent subjects’ confidence level in predicting risky behaviors and show how metacognition in theory of mind for prediction of others’ choices is represented in the brain’s activity.

Keywords: Confidence Level; Prediction; Metacognition; Decision-Making.

1. Introduction

Previous studies have shown that confidence in decision-making and value-based decision-making tasks [1- 3] have been represented in the activity of prefrontal cortex. Moreover, our confidence in prediction of others' choices is less investigated, though there are studies in the domain of predicting others' decisions [4]. This experimental design uses functional Magnetic Resonance Imaging (fMRI) combined with a risky decision-making task to investigate the active brain regions correlated with participants' confidence in prediction of others' risky decision making.

2. Materials and Methods

Using a 3T fMRI scanner, we scanned 21 (10 females) healthy and normal participants with an age range between 22 and 29 (average of 24.6). The experimental task consists of three runs in two sessions. In the first runs, participants repeatedly choose between two monetary reward options for themselves in 39 trials, a risky and sure options. Participants predict a stranger's (observee) choices in the second run and simultaneously report their confidence within the scale of two (Figure 1). Lastly, the third runs contain a combination of the first and the second runs. The experiment is performed in two separate sessions with the same structure. In this study, we specifically focus on the second run of each session to find active areas that represent the confidence in prediction of observee.

Before the experiment, participants were told the choices they observed in prediction trials were made by two real people (one person in each session) who had previously participated. But in fact, the observee choices are generated by computer algorithms (one risk-seeker and the other risk-averse). With counterbalancing, each observee was randomly assigned to the first or second session of the experiment.

For fMRI data preprocessing, FMRIB Software Library (FSL) is used for slice timing correction, motion correction, spatial smoothing (8-mm full width at the half maximum), high-pass temporal filtering (filter width of the 100s), and field map correction. Moreover, Advanced Normalization Tools (ANTs) was used to achieve accurate registration. After preprocessing, a Generalized Linear Model (GLM) was applied to the fMRI data to calculate beta values and ultimately find the active brain regions based on different contrasts.

3. Results

Using fMRI, we find that the activities in the frontal pole cortex (FPC), cingulate gyrus, and precuneus cortex ($P < 0.0005$; cluster size, $k > 75$) reflect more variation in participants' confidence level (high confidence less confidence contrast) while predicting others' decisions (Figure 2A). In the behavioral data, a higher confidence level correlated with more accuracy in predictions (Figure 2B). When participants answer correctly, their confidence level as a metacognition factor increases simultaneously and vice versa. This correlational relation can represent the metacognitive processes during the task.

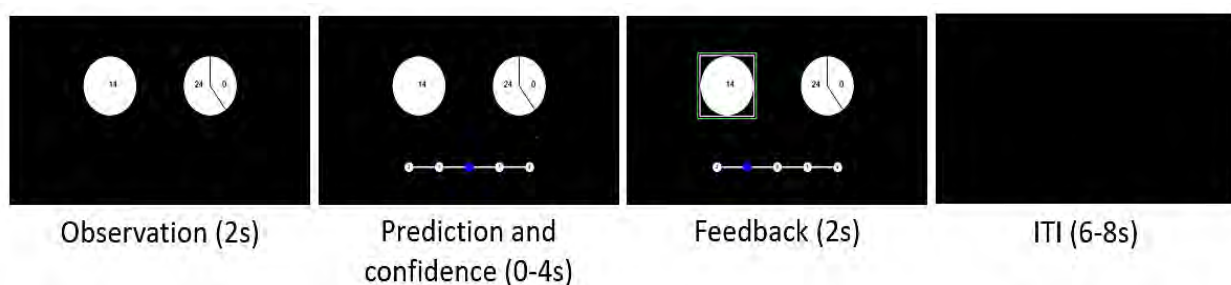


Figure 1. Experiment task paradigm. In the observation phase, risky and sure choices are demonstrated to participants, and after prediction with a two-scale confidence level, true choice is given as feedback

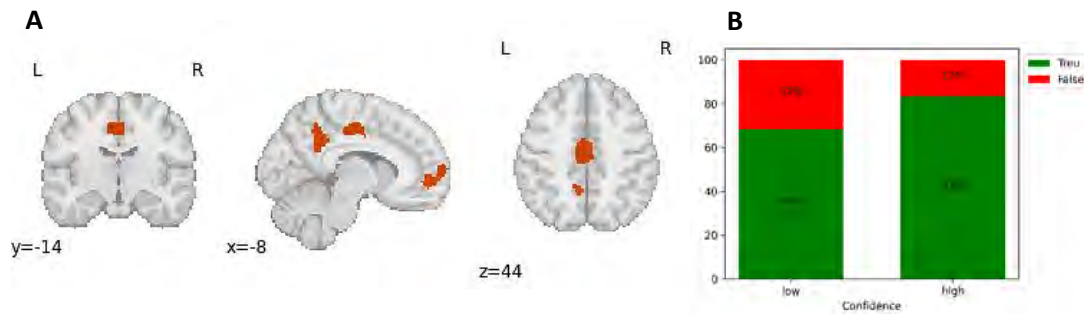


Figure 2. FMRI and behavioral results for confidence level. (A) Neural representation of higher confidence level when predicting others' behavior. (B) Prediction accuracy in low and high confidence trials

4. Conclusion

Confidence levels in decision-making conditions remain a trending topic in metacognition studies. Our finding indicates a positive correlation between confidence level as a metacognitive factor and choice accuracy in predicting others' choices. The importance of this confidence representation is its social context and it can be considered as metacognition on the theory of mind; because during the task, subjects try to read the mind of other people and predict their decisions. This type of metacognition plays a crucial role in social interactions and can show distinct activity relative to metacognition studies on perceptual or mnemonic decision-making. Future studies are needed to compare these different types of decision-making with social decision-making.

References

- 1- De Martino, B., Fleming, S. M., Garrett, N., & Dolan, R. J. "Confidence in value-based choice." *Nature neuroscience*, 16(1), 105-110. Srisatkunarajah, S. and Jeyakumar, V., Multiaxial Fatigue, F. Tinakoe and M. Lukus (Editors), Prentice Hall, 1985, pp. 240-252, (2013).
- 2- Fleming, S. M., Huijgen, J., & Dolan, R. J. "Prefrontal contributions to metacognition in perceptual decision making.", *Journal of Neuroscience*, 32(18), 6117-6125, (2012).
- 3- Barron, H. C., Garvert, M. M., & Behrens, T. E. "Reassessing VMPFC: full of confidence?." *Nature neuroscience*, 18(8), 1064-1066, (2015).
- 4- Suzuki, S., Jensen, E. L., Bossaerts, P., & O'Doherty, J. P. "Behavioral contagion during learning about another agent's risk-preferences acts on the neural representation of decision-risk.", *Proceedings of the National Academy of Sciences*, 113(14), 3755-3760, (2016).



Joint Modeling of Structural-Functional Brain Networks in Full-Term Neonates

Mahshid Fouladivanda ¹ , Kamran Kazemi ¹, Habibollah Danyali ¹, Ardalan Aarabi ^{2,3}

¹ Department of Electrical and Electronics Engineering, Shiraz University of Technology, Shiraz, Iran

² Laboratory of Functional Neuroscience and Pathologies (LNFP UR4559), University Research Center, University Hospital, Amiens, France

³ Faculty of Medicine, University of Picardy Jules Verne, Amiens, France

*Corresponding Author: Mahshid Fouladivanda
Email: m.fouladivanda@sutech.ac.ir

Abstract

The structural and functional organization of the human brain in early stages of neurodevelopment are largely unknown due to drastic changes in brain function and structure. In neonates, most previous studies have investigated the brain connectome using resting-state functional Magnetic Resonance Imaging (rs-fMRI) and/or Diffusion Weighted Imaging (DWI). The relationship between the neonatal structural and functional brain networks is still a matter of debate and controversy. In this study, we present a modified joint modeling approach based on topological learning algorithms originally introduced in [1], to integrate functional and structural brain networks in full-term neonates. The approach was evaluated on synthetic and real imaging data from the developing Human Connectome Project (dHCP) dataset. Using our joint structural-functional approach, we were able to better identify true connections in comparison with the original joint model.

Keywords: Joint Structural Functional Network; Resting State Network; Full-Term Neonate.

1. Introduction

In the past decade, advances in network science have allowed scientists to better characterize the functional and structural organization of the human brain. In recent years, brain connectivity analysis has gained increasing attention to characterize the architecture of human brain networks [1]. The majority of previous studies have explored brain functional or structural networks using single modalities including rs-fMRI or DWI [2]. Investigation of the relationship between the structural and functional brain networks has become a point of focus for scientists. Recently a joint structural-functional model was introduced based on information flow between different functional regions by physical paths [1]. In this study, we present an improved joint modeling approach by taking into account the topology of both structural and functional brain networks using DWI and rs-fMRI data from neonates. In this model, the connectivity between functional brain modules is directly learned from both structural and functional interactions. Functional modules were also determined based on resting state network analysis using rs-fMRI.

2. Materials and Methods

In our study, we used the DWI phantom data (FiberCup, 3 mm isotropic, 64 directions uniformly distributed over the sphere, with $b = 2000$) [3], a dMRI dataset with identified fiber paths (ground truth), and synthetic functional data provided in [1] to evaluate the proposed model. We further trained and evaluated the method using the DWI and 15-min rsfMRI data from 40 term neonates (aged 37- 44 weeks GA) included in the developing human connectome project, dHCP, (<http://www.developingconnectome.org/>). The DWI and rsfMRI data were minimally preprocessed by dHCP. Then, we performed deterministic fiber tractography using the Euler tracking algorithm by the DSI-studio software (<http://dsi-studio.labsolver.org/>) [4].

Phantom data: To construct the structural/functional networks, we first defined 16 parcels defined in the dataset. Then, the structural connectivity map was constructed by performing tractography using the phantom DWI data. The synthetic functional connectivity and functional module activation were also provided in [1].

Experimental data: First, the functional parcellation was performed by the spatially-constrained Normalized-Cut (NCUT) spectral clustering algorithm [5] based on the AAL atlas with 900 parcels using preprocessed rs-fMRI data. A Structural Connectivity matrix (SC) was then constructed for each neonate. Then, the structural connections across at least 60% of all the neonates were kept and others were removed to obtain the binary group-level (backbone) SC matrix. A group functional connectivity matrix was also computed by averaging connection weights over all neonates. In addition, a group independent component analysis [6] was performed to identify Independent Components (ICs) grouped into eight resting state networks used as functional modules.

Main algorithm: For joint modeling, we first determines a topological brain connectivity network based on both structural and functional connections. For this purpose, the topological information was obtained by an optimized learning algorithm using the method described in [7]. Then, we performed the joint linear modeling based on the method introduced in [1] to find the interaction between different functional modules using the topological learning network.

3. Results

Table 1 presents the results of our model in comparison with the original method. As shown, our model was able to find more true connections. Our method also resulted in reduced number of missed connections in comparison with the original model [1].

Table 1. Evaluation results compared to the ground truth

Scheme	False Connections	Missing Connections	True Connections	Dataset
Ground Truth	-	-	24	Phantom DWI
Joint Brain Network Model [1]	1	18	6	Phantom DWI + rs-fMRI
Proposed Method	2	13	11	Phantom DWI + rs-fMRI

Figure 1 illustrates the graphs of the structural, functional, topological, and joint modeling networks of the neonatal brain.

In this representation, the color-coded brain networks in each functional module have stronger connections.

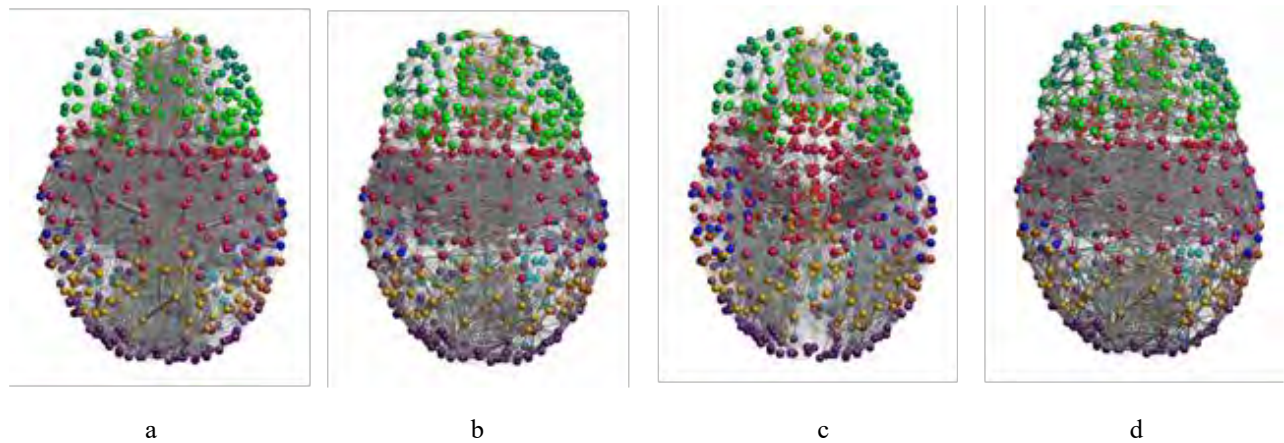


Figure 1. Graph representation of the structural (a), functional (b), topological (c), and joint proposed (d) networks

4. Conclusion

Our findings indicate cross linking between the structural and functional connections of human brain network in neonates.

Acknowledgment

This work was partially supported by the Cognitive Science and Technology Council (CSTC) of Iran under the grant numbers 8473.

References

- 1- S.-H. Chu, K. K. Parhi, and C. Lenglet, "Function-specific and enhanced brain structural connectivity mapping via joint modeling of diffusion and functional MRI." *Sci. Rep.*, vol. 8, no. 1, pp. 1–19, (2018).
- 2- D. Zhu *et al.*, "Fusing DTI and fMRI data: a survey of methods and applications." *Neuroimage*, vol. 102, pp. 184–191, (2014).
- 3- C. Poupon, B. Rieul, I. Kezele, M. Perrin, F. Poupon, and J. Mangin, "New diffusion phantoms dedicated to the study and validation of high-angular-resolution diffusion imaging (HARDI) models." *Magn. Reson. Med. An Off. J. Int. Soc. Magn. Reson. Med.*, vol. 60, no. 6, pp. 1276–1283, (2008).
- 4- F. C. Yeh, T. D. Verstynen, Y. Wang, J. C. Fernández-Miranda, and W. Y. I. Tseng, "Deterministic diffusion fiber tracking improved by quantitative anisotropy." *PLoS One*, vol. 8, no. 11, p. e80713, (2013), doi: 10.1371/journal.pone.0080713.
- 5- R. C. Craddock, G. A. James, P. E. Holtzheimer, X. P. Hu, and H. S. Mayberg, "A whole brain fMRI atlas generated via spatially constrained spectral clustering." *Hum. Brain Mapp.*, vol. 33, no. 8, pp. 1914–1928, (2012), doi: 10.1002/hbm.21333.
- 6- V. D. Calhoun, T. Adali, G. D. Pearlson, and J. J. Pekar, "A method for making group inferences from functional MRI data using independent component analysis." *Hum. Brain Mapp.*, vol. 14, no. 3, pp. 140–151, (2001), doi: 10.1002/hbm.1048.
- 7- T. Songdechakraiwit and M. K. Chung, "Topological learning for brain networks." *arXiv Prepr. arXiv2012.00675*, (2020).



Electroencephalographic Microstates Analysis in Major Depressive Disorder

Vahid Asayesh ^{1*} , Mehdi Dehghani ¹, Majid Torabi ¹, Sepideh Akhtari ¹, Tomas Ros ^{2,3}

¹ NPCindex Research Company

² Department of Fundamental Neuroscience, Functional Brain Mapping Laboratory, Campus Biotech, University of Geneva, Geneva 1202, Switzerland

³ Lemanic Biomedical Imaging Centre, Geneva 1202, Switzerland

*Corresponding Author: Vahid Asayesh
Email: Vahid.asayesh@gmail.com

Abstract

Microstates suggest a promising framework to investigation brain dynamics in the resting state Electroencephalography (EEG). In this paper, microstate based measures including occurrence, mean duration, and time coverage were compared between depressed and healthy subjects using broadband (1-30 Hz) and frequency-specific decomposition. The results show that in delta and theta frequency bands, microstate B has significantly shorter mean duration (delta: $p = 0.008$, $d = 0.80$, theta: $p = 0.05$, $d = 0.56$) and coverage (delta: $p = 0.03$, $d = 0.63$, theta: $p = 0.04$, $d = 0.58$) in healthy subjects. Also, in delta frequency band, microstate C occurred significantly less frequently ($p = 0.004$, $d = -0.86$) with low coverage ($p = 0.01$, $d = -0.70$) in depressed patients.

Keywords: Major Depressive Disorder; Electroencephalography; Microstates; Depression Biomarkers.

1. Introduction

Major Depressive Disorder (MDD) is among the most serious psychiatric disorders and the main source of disability. Electroencephalography (EEG) measures electrical activity of the brain and is one of the widely used modalities in depression research. EEG presents good temporal resolution thus it is suitable for studying complex brain functions and can provide information that is difficult to obtain using other imaging modalities. Most of the studies in the depression field, used power spectra, frequency domain, or statistical features of EEG signal. Such features have failed to utilize the high temporal resolution advantage of EEG. Lehmann *et al.* [1] observed that in resting-state EEG, the topography of the scalp potential map remains stable for a short period of time (80-120 ms) and then switches to a new topography which remains stable again. They called these short periods of stability EEG microstates and attributed them to periods of synchronized activity within large-scale brain networks. Studies on EEG microstates showed altered temporal characteristics of microstates in depressive patients compared to healthy subjects. Authors in [2,3] showed unchanged numbers of different microstates per second but abnormal microstate topographies and reduced overall average microstate duration in depressive subjects. Atluri *et al.* [4] reported increase in overall microstate duration and decrease in overall microstates occurrence per second in treatment-resistant depression. Dumborska *et al.* [5] demonstrated that depressive and healthy groups did not differ in any temporal parameter including occurrence, coverage, and duration in any microstate. Results of [6] illustrated that microstate D covered a greater proportion of the recording in the healthy group than MDD group. Also, this microstate had a higher average occurrence and average duration in healthy group. Although these studies have been able to link the temporal characteristics of EEG microstates to depression disorder, they have overlooked the effect of different EEG frequency bands in their analysis. Therefore, the aim of this paper is to investigate the temporal dynamics of EEG microstates in delta, theta, alpha, and beta frequency bands in depressive disorder.

2. Materials and Methods

In this study, EEG signal was acquired from 24 MDD patients (mean of age: 37.50 ± 13.62 years old) and 24 healthy subjects (mean of age: 32.99 ± 7.73) who were referred to the Asayesh rehabilitation clinic, Tabriz, Iran. In each group 50% of the subjects are

female and 50% of them are male. The diagnosis of MDD was made based on DSM-V criteria by an expert psychiatrist. All of the subjects were medication-free. The EEG signal was recorded from participants for 5 minutes in Eyes Closed (EC) condition according to 10-20 international system using Mitsar 19 channel device. Low pass, high pass, and notch filters were used to clean up the signals. Then, Infomax independent component analysis (ICA) was applied to remove ocular artifacts. The de-noised dataset was parsed into broadband (1-30 Hz), delta (1-4 Hz), theta (4-8 Hz), alpha (8-12 Hz), and beta (15-30 Hz) frequency bands. EEG microstates were estimated initially at the single-subject level from each frequency band using polarity-independent k-means ($k = 4$) clustering to derive four microstate maps (A, B, C, and D). Single-subject maps were then re-ordered by minimizing the average spatial correlation across maps. Next, microstate maps were averaged across all subjects group-wise, obtained in a series of group-averaged maps. Finally, grand mean maps were fitted back to the single-subject data. Microstates spatiotemporal measures including occurrence, mean duration, and time coverage were then computed at the single-subject level [6].

Three microstate measures were compared between groups with different frequency band microstate maps using an independent t-test ($\alpha \leq 0.5$) to show the p-value and Cohen's D (d) was reported as the effect size for each test.

3. Results

According to Figure 1, broadband, alpha, and beta frequency bands microstates characteristics don't show any significant differences between MDD and healthy subjects. Delta frequency band microstate B shows higher duration and coverage in MDD patients. Microstate C in delta frequency band has less occurrence and coverage in MDD subjects than healthy subjects. Also, Theta frequency band microstate B has significantly higher duration and coverage in depressed group.

4. Conclusion

This paper investigates temporal features of frequency-specific EEG microstates ability in

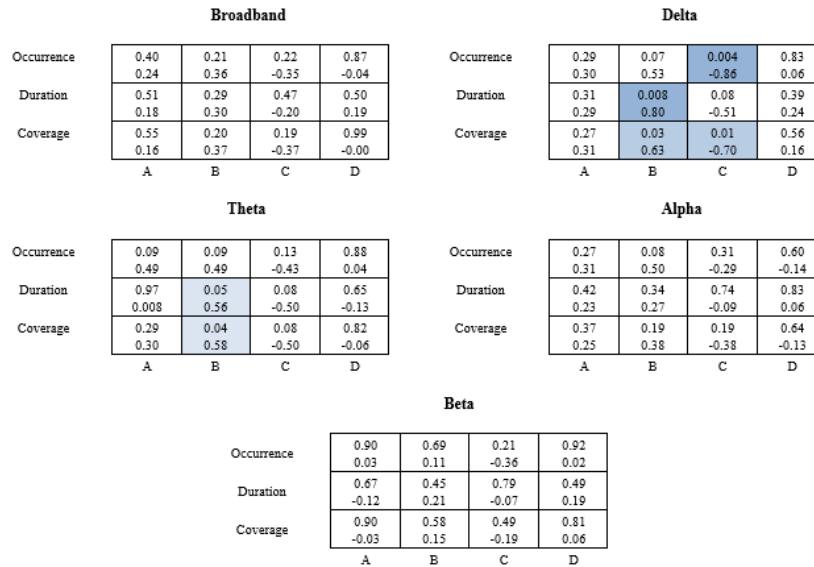


Figure 1. P-value and Cohen’s D values for different frequency bands microstates using occurrence, duration, and coverage features. The first number is the p-value and the second number is Cohen’s D

distinguishing MDD and healthy subjects. In conclusion, microstates in delta and theta frequency bands show significant differences between two groups. In these frequency bands, microstate B has a higher duration and coverage in MDD patients while microstate C has higher occurrence and coverage in healthy subjects.


6- M. Murphy, *et al.*, “Abnormalities in electroencephalographic microstates are state and trait markers of major depressive disorder,” *Neuropsychopharmacology*, 45(12), 2030–2037, (2020).

References

- 1- D. Lehmann, *et al.*, “EEG alpha map series: brain micro-states by space-oriented adaptive segmentation.” *Electroencephalogr Clin Neurophysiol*, 67:271–88, (1987).
- 2- W. K. Strik, *et al.*, “Larger topographical variance and decreased duration of brain electric microstates in depression.” *J Neural Transm*, 99:213–22, (1995).
- 3- R. Ihl, J. Brinkmeyer, “Differential diagnosis of aging, dementia of the Alzheimer type and depression with EEG-segmentation,” *Dement Geriatr Cogn Disord*, 10:64–9, (1999).
- 4- S. Atluri, *et al.*, “Selective modulation of brain network dynamics by seizure therapy in treatment-resistant depression.” *NeuroImage Clin*, 20:1176–90, (2018).
- 5- A. Damborská, *et al.*, “EEG resting-state large-scale brain network dynamics are related to depressive symptoms.” *Frontiers in Psychiatry*, 10 548, (2019).



Structural and Functional Connectivity Analysis in Cannabis Users

Najme Soleimani ^{1*} , Kamran Kazemi ¹, Sara Jafakesh ¹, Mohammad Sadegh Helfroush ¹, Valentina Lorenzetti ², Ardalan Aarabi ^{3,4}

¹ Department of Electrical and Electronics Engineering, Shiraz University of Technology, Shiraz, Iran

² Neuroscience of Addiction and Mental Health Program, Healthy Brain and Mind Research Centre, Australian Catholic University, Melbourne, Australia

³ Laboratory of Functional Neuroscience and Pathologies, University Research Center, University Hospital, Amiens, France

⁴ Faculty of Medicine, University of Picardie Jules Verne, Amiens, France

*Corresponding Author: Najme Soleimani
Email: N.Soleimani@sutech.ac.ir

Abstract

Cannabis is one of the most used and commodified illicit substances worldwide, especially among adolescents. Heavy cannabis use has been associated with aberrant neurobiology. The precise mechanisms of cannabis are yet to be identified particularly in youth due to low sample sizes and a low number of studies being conducted, and a focus on distinct brain integrity. The purpose of this study is to concurrently measure brain structural and functional connectivity in cannabis users using resting state functional Magnetic Resonance Images (rs-fMRI) and Diffusion Weighted Images (DWI), for a comprehensive characterization of structural and functional neurobiology. The rich club organization of structural and functional brain networks will be further investigated using a cohort of 1206 young adults (age 22-36, 54% female) from Human Connectome Project (HCP). We evaluate our framework on a group of 73 cannabis users (age 22-36, 19 female) in comparison with 73 healthy controls (age 22-36, 14 female).

Keywords: Cannabis; Functional Connectivity; Structural Connectivity; Rich Club.

1. Introduction

Cannabis use is associated with a wide variety of psychiatric disorders, especially when heavy cannabis is used during adolescence, such as risky behaviors, lack of motivation, increased risk of cannabis use disorders and psychosis [1]. Several neuroimaging network studies have assessed brain functional and structural connectivity associated with chronic cannabis use using resting state functional and diffusion weighted imaging data [2,3]. Structural connectivity assesses the existence of fiber tracts in the white matter between different anatomically connected brain regions; whilst functional connectivity is defined based on the spontaneous co-activation patterns of brain [3]. In recent years, there has been growing interest in identifying densely connected hubs (so-called “rich club”) shown to play a critical role in information integration in structural and functional brain networks [4]. In this study, we explored alterations in brain functional and structural connectivity and the rich club organization of structural and functional brain networks using graph theoretical metrics in cannabis users in comparison with healthy controls well matched with cannabis group on age, sex, education, BMI, alcohol and tobacco usage.

2. Materials and Methods

Participants: The participants in this study were selected from the young adult HCP final release (<https://www.humanconnectome.org/study/hcp-young-adult/document/1200-subjects-data-release>). From this large cohort, 109 individuals met the DSM-IV criteria for cannabis dependence and had both rs-fMRI and DWI imaging data. From this subgroup, individuals with comorbid alcohol dependence, outliers on DSM levels of anxiety and depression (>3 SD from the mean of all 1206 HCP subjects) in addition to those individuals with low quality outlier images were excluded [5]. The final sample included 73 cannabis users. The healthy control group was selected from healthy subjects well matched with the cannabis group on age, sex, education, BMI, alcohol and tobacco usage.

Parcellation scheme: The HCP multimodal parcellation (<https://balsa.wustl.edu/file/87B9N/>) was used as the parcellation scheme. The cortical surface was parcellated into 360 regions using Glasser atlas [6]. As the subcortical regions are predominant in the studies of addiction, 19 subcortical regions were added from

FreeSurfer (<https://surfer.nmr.mgh.harvard.edu/>), which resulted in 379 parcels in total.

Structural and functional Networks: The HCP imaging data were acquired on a Siemens 3T scanner (TR/TE= 0.72 ms/ 0.33 ms, T=1200 frames). The rs-fMRI data were acquired in 4 runs of approximately 15 min each. The dMRI sessions (TR/TE= 5520 ms/89.5 ms) included 6 runs and 3 different shells of b=1000, 2000 and 3000 s/mm². The rs-fMRI and dMRI data were minimally processed according to the standard preprocessing pipeline [7]. The tractography for each individual was computed using the deterministic generalized Q-sampling imaging (GQI) fiber tracking algorithm by DSI Studio software (<http://dsi-studio.labsolver.org/>). For each participant, we constructed a structural connectivity matrix, whose elements represented the normalized QA between regions. A functional connectivity matrix also was constructed for each individual by calculating the Pearson's correlation coefficient of the average time courses between each pair of 379 regions by using connectome workbench platform (<https://www.humanconnectome.org/software/connectome-workbench/>). A weighted group structural matrix was computed for each group by averaging the individual matrices elements for those connections present in at least 75% of the unweighted individual matrices [8]. A binary group functional matrix was also computed for both groups by averaging the individual matrices by preserving 20% of the strongest connections. From the connectivity matrices in the individual and group level, the topological graph metrics including degree, clustering coefficient, local and global efficiency, path length, and modularity were estimated.

A rich club in a complex network can be described as a set of high degree, densely-interconnected nodes. Rich club analysis was performed on the group connectivity matrices in order to study alteration in the rich club organization of structural and functional brain networks in cannabis users in comparison with control group as well as the overlap of functional and structural rich clubs. Furthermore, we used regression analysis to examine the relationship between network measures and times used marijuana of cannabis users (p-value <0.05, uncorrected).

3. Results

We found no significant differences in global or regional metrics of structural and functional networks; although, we found statistically significant weaker structural and

functional connections between regions including amygdala, auditory association cortex or inferior parietal cortex in cannabis users compared with healthy controls. Several significant associations were observed in the investigation of potential link between times used marijuana and network measures using regression analysis; for instance, parameters such as degree or clustering coefficient indicated negative association with times used marijuana in some regions such as parahippocampal area and entorhinal cortex.

In terms of rich club analysis, structural rich club included nodes mostly within temporal and frontal regions, while functional rich club nodes were mostly in occipital and temporal regions. The minor differences were seen in rich club organizations (Figure 1).

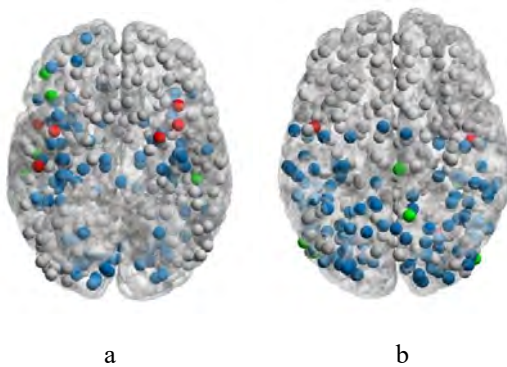


Figure 1. Rich club organization of (a) structural network and (b) functional network for cannabis users and healthy controls. The similar rich club nodes in two groups, rich club nodes that exist just in healthy controls and rich club nodes that exist just in cannabis users are shown in blue, red and green, respectively

4. Conclusion

In this study, graph theoretic analysis was performed on whole-brain functional and structural networks of CB users and healthy controls in order to identify brain regions and connections associated with cannabis use. These findings suggest minor effects on regional segregation and integration network parameters.

Acknowledgment


This project was supported by the Cognitive Science and Technology Council (CSTC) of Iran under the grant number 9336.

References

- 1- P. Manza, D. Tomasi, and N. D. Volkow, "Subcortical Local Functional Hyperconnectivity in Cannabis Dependence." *Biol. Psychiatry Cogn. Neurosci. Neuroimaging*, vol. 3, no. 3, pp. 285–293, (2018), doi: 10.1016/j.bpsc.2017.11.004.
- 2- D. J. Kim *et al.*, "Structural Network Topology Revealed by White Matter Tractography in Cannabis Users: A Graph Theoretical Analysis." *Brain Connect.*, vol. 1, no. 6, pp. 473–483, (2011), doi: 10.1089/brain.2011.0053.
- 3- M. M. G. Koenis *et al.*, "Associations of cannabis use disorder with cognition, brain structure, and brain function in African Americans." *Hum. Brain Mapp.*, vol. 42, no. 6, pp. 1727–1741, (2021), doi: 10.1002/hbm.25324.
- 4- D. J. Kim *et al.*, "Aberrant structural–functional coupling in adult cannabis users." *Hum. Brain Mapp.*, vol. 40, no. 1, pp. 252–261, (2019), doi: 10.1002/hbm.24369.
- 5- P. Manza, E. Shokri-Kojori, and N. D. Volkow, "Reduced Segregation between Cognitive and Emotional Processes in Cannabis Dependence." *Cereb. Cortex*, vol. 30, no. 2, pp. 628–639, (2020), doi: 10.1093/cercor/bhz113.
- 6- M. F. Glasser *et al.*, "A multi-modal parcellation of human cerebral cortex." *Nature*, vol. 536, no. 7615, pp. 171–178, (2016), doi: 10.1038/nature18933.
- 7- M. F. Glasser *et al.*, "SC a Department." *Neuroimage*, (2013), doi: 10.1016/j.neuroimage.2013.04.127.
- 8- M. P. Van Den Heuvel and O. Sporns, "Rich-Club Organization of the Human Connectome." vol. 31, no. 44, pp. 15775–15786, (2011), doi: 10.1523/JNEUROSCI.3539-11.2011.



The Causal Role of the Lateral Intraparietal Area in Object Long-Term Value Memory

Leila Noorbala¹, Reza Khosrowabai¹, Omid Sharafi², Ali Ghazizadeh^{2*} 

¹Institute for Cognitive and Brain Sciences, Shahid Beheshti University, Tehran, Iran

²Bio-Intelligence Unit, Electrical Engineering Department, Sharif University of Technology, Tehran, Iran

*Corresponding Author: Ali Ghazizadeh
Email: ghazizadeh@sharif.edu

Abstract

Our lives are cluttered with loads of information; however, we are still able to attend to cues that signal future rewards. Previous studies have implicated the Lateral Intraparietal cortex (LIP) in encoding objects' reward history. Here, we investigated the causal role of LIP in the long-term value memory of objects by creating virtual lesions using Theta-Burst Stimulation (cTBS) in human subjects. 18 healthy subjects were trained to assign monetary values to 32 abstract visual stimuli (fractals). During value training, subjects were trained with two sets of objects before and two sets after the LIP lesion. A day later, during the value retrieval task, subjects had to judge the value of each object as good or bad (single object choice). For the sets that were trained before the LIP lesion, the performance was above 70% and slightly better for good compared to bad. Interestingly, for the post-lesion sets, there was a better memory for bad compared to good objects on the contralateral side, with a stronger effect size for the right side suggesting an asymmetry in the role of LIP. Notably, the performance of sets pre- and post-lesion during the learning was not different. These results show a selective effect on wiping object's long-term memory by LIP lesion and pave way for disrupting maladaptive object reward memories observed in cue-driven addictive behavior.

Keywords: Value Memory; Lateral Intraparietal Area; Continuous Theta Burst Stimulation.

1. Introduction

Despite being constantly bombarded by environmental input, humans can still attend to and retrieve valuable objects. The concept of value is one of the most critical aspects of prioritizing objects based on their reward history. The brain must compute a value signal to evaluate which action leads to a rewarding outcome to make optimal decisions [1]. The selection of these objects is based on the brain's ability to retain the value of objects over time, known as long-term value memory [2]. The misdirection of value-based memories has a significant role in maladaptive behavior, such as addiction. Addiction is characterized by persistent maladaptive memories that are resilient to extinction and maintain drug-seeking [3].

Previous studies have implicated the role of the Lateral Intraparietal area (LIP), a subdivision of the Inferior Parietal Lobule (IPL), in encoding objects' reward history in non-human primates [4]. They found a pronounced long-term value memory in core subregions of the temporal and prefrontal cortex, including LIP, that maintains rewarding object discrimination over a long period which is critical for using learned value memory to direct goal-oriented behavior. Also, a recent fMRI study demonstrates neural correlates of value memory, one of which is LIP. It activates by rewarding objects than no rewarding ones, days after the final reward training session, and in the absence of rewards in human subjects (Farmani *et al.*, 2022). On the other hand, long-term value memory can be modulated via a reconsolidation process triggered by conditioned stimulus exposure [5]. By way of illustration, memory manipulation after retrieval has received attention for its therapeutic potential to change memory expression.

Along the same lines, we propose a non-pharmacological intervention method that selectively interferes with object long-term value memory, which may pave the way for disrupting maladaptive object reward memories observed in cue-driven addictive behavior. In this study, we investigate whether the involvement of the LIP area in object value long-term memory is causal or the memory-related activity in LIP is due to the feedback from other brain regions that contribute to the primary process. To address the causal role of LIP, we have created virtual lesions over it using Theta-Burst Stimulation (cTBS) in human subjects. We hypothesize that temporary inactivation of the LIP region interferes with Object Long-Term Value Memory in human subjects. In other words, LIP inactivation causes a reduction of contralesional value

memory. Since each hemisphere controls opposite visual hemifield, we expect that unilateral LIP inactivation induces a decline of value memory only for contralesional hemifield objects. Hence, we inactivate each LIP respectively for a distinct group of subjects and present each stimulus exclusively in a contralesional or ipsilesional hemifield to test how LIP inactivation affects the value memory of the contralesional hemifields objects.

2. Materials and Methods

Eighteen healthy adult subjects aged from 20 to 40 with normal or corrected-to-normal vision have participated in the study for two consecutive days. The first day was an object-value learning day through which they were trained to assign monetary values to 32 abstract visual stimuli (fractals). The parameters determining each stimulus' color, size, and edge were randomly assigned. Half of the Fractals were randomly assigned to high reward (good object) and the other half to no reward groups (bad objects); moreover, the assignment of stimuli into the two groups was also random for each subject during the training phase. The stimuli were presented exclusively in the right or left hemispheres, with the intention to have half of the stimuli delivered in contralesional hemifields after unilateral lip inactivation and the other half in ipsilesional hemifields. In general, each subject was trained to assign monetary values to 32 fractals that fell into one of the four categories: good-left, good-right, bad-left, and bad-right.

Each subject is trained in one session to learn the object-value associations using Psychtoolbox extensions via MATLAB. Each session consists of four runs, with each run consisting of eight stimuli (4 good/4 bad) and a total of 96 trials. There are 48 force trials and 48 choice trials randomly distributed among the force ones in the training phase. Participants were instructed to learn the object-value associations through force and choice trials intermixed. To investigate the learning of the subjects. Each force trial starts with a white fixation point at the center of a black screen. After 800 milliseconds, one of the fractal stimuli is presented to either left or right side of the fixation. Then, the fractal and fixation point remain for 1 second and 200 milliseconds on the screen; subjects should not make a saccade toward the fractals until the fixation point disappears. We have an eye tracker to

make sure this condition is achieved. The feedback is presented to the subjects for 1 s following the response. Correct and fast responses to good objects receive 5000 tomans and a correct tone. In unitary-choice trials, participants were asked to evaluate the fractal value, to investigate the learning of the subjects. Another type of choice trial is the binary choice trial, in which subjects were asked to choose one of the two objects which have the higher value. The feedback is delivered for 1 second after the response to boost the respondents' engagement with the task.

During value training, subjects were trained with four sets of objects, two of which were before and the other two sets after unilateral LIP inactivation. The LIP area was reversibly inactivated using Transcranial Magnetic Stimulation (TMS), a non-invasive brain stimulation technique. TMS device generates a magnetic field around the skull, by passing a varying current through a magnetic coil. The time variation of the magnetic field induces an electric field in the brain tissue, which induces an electrical current in the intracellular and extracellular space, causing cell membranes to become depolarized or hyper-polarized. Continuous Theta-Burst Stimulation (cTBS) is an advanced form of repetitive TMS involving a burst of three stimuli at 50 Hz repeated at 5-Hz intervals. Administering cTBS induces a transient disruption of cortical activity during task performance called a virtual lesion which is used to explore causal brain-behavior relations. We employed the cTBS600 protocol over the LIP, which has an after-effect duration of about 20 minutes to 1 hour [6]. The LIP region has been marked based on each Subject's T1-Weighted MRI to target TMS pulses accurately through real-time mapping guided by navigated TMS. We created a virtual lesion on the right LIP for the first group of patients and on the left LIP for the second group to explore the effect of unilateral LIP inactivation on contralesional hemifields objects.

Twenty-four hours later, on the second day, the value retrieval task was performed by the unitary choice trials to examine the value-based memory of the participants. Subjects had to judge the value of each pre-trained LIP lesion and post-train LIP lesion sets which half of them were presented contralesional and the other half ipsilesional, as good or bad.

3. Results

The accuracy of unitary choice trials is computed before and after LIP inactivation on the first day for the ipsilesional and contralesional hemifields for both good and bad objects to assess the subjects' value learning. During unitary choice trials, the performance of pre and post-lesion sets is around 85% for good objects in both contralesional and ipsilesional hemifields objects (Figure 1). Interestingly, the performance of pre and post-lesion sets during the learning trials does not vary significantly.

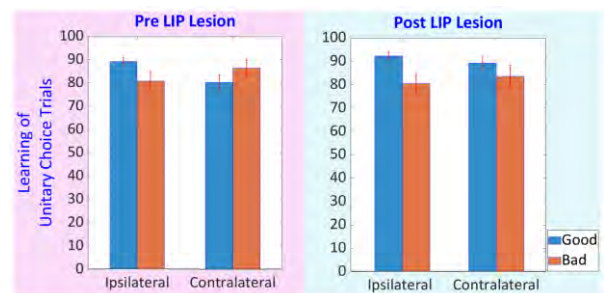


Figure 1. Accuracy of Unitary Choice Trials in Learning Task

To address the value-based memory of the participants, The subjects' accuracy is computed on the second day before and after LIP inactivation for the objects presented in ipsilesional and contralesional hemifields. The behavioral performance shows that for the sets trained prior to LIP lesion, the commission for good objects is above 75% for all good objects presented in both hemifields. In contrast, the performance of value memory of good contralesional hemifields objects after LIP lesion was around 60% (Figure 2). At the same time, there was no significant difference between pre and post-lesion good ipsilesional hemifields objects. Suggesting selective value memory alteration after cTBS over LIP only for four good fractals presented on the contralesional hemifield out of 32 fractals.

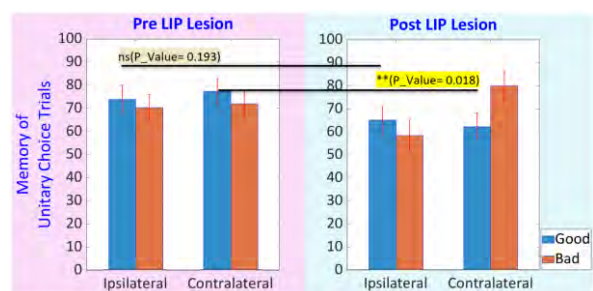


Figure 2. Accuracy of Unitary Choice Trials in Memory Task

Furthermore, on the second day, the performance is slightly better for good compared to bad objects for sets trained prior to LIP lesion in both hemifields. In contrast, there is a better memory for bad than good objects on the contralesional hemifield for the post-lesion sets (Figure 3). It suggests that after inactivating the LIP, the subjects rated the contralesional hemifields objects as bad ones with a higher probability. However, subjects reported greater confidence in judging the value of the objects learned after LIP inactivation than before during the value retrieval task.

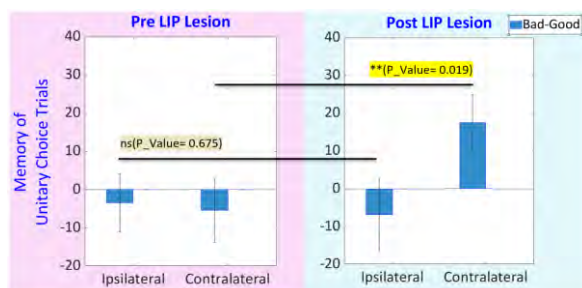


Figure 3. Difference in Memory Task Performance Between Good and Bad Objects

4. Conclusion

Here, we investigated the causal role of LIP in the long-term value memory of objects and hypothesized that creating virtual lesions over the LIP area selectively disrupts the memory of the objects that were presented in contralesional hemifield. Results show a selective effect on wiped objects from the long-term memory by LIP lesion. The present findings authenticate those temporary lesions over LIP using continuous theta-burst stimulation causing a reduction of long-term value memory for the objects presented in contralesional hemifield in humans. At the same time, the cTBS over LIP has no impact on the learning of the objects-value association. These may open new frontiers in treating maladaptive object reward memories observed in cue-driven addictive behavior.

Acknowledgment

The authors wish to National Brain Mapping Laboratory (NBML), Tehran-Iran, for providing the data acquisition.

References

- 1- P. Manza, D. Tomasi, and N. D. Volkow, "Subcortical Local Functional Hyperconnectivity in Cannabis Dependence." *Biol. Psychiatry Cogn. Neurosci. Neuroimaging*, vol. 3, no. 3, pp. 285–293, (2018), doi: 10.1016/j.bpsc.2017.11.004.
- 2- D. J. Kim *et al.*, "Structural Network Topology Revealed by White Matter Tractography in Cannabis Users: A Graph Theoretical Analysis." *Brain Connect.*, vol. 1, no. 6, pp. 473–483, (2011), doi: 10.1089/brain.2011.0053.
- 3- M. M. G. Koenis *et al.*, "Associations of cannabis use disorder with cognition, brain structure, and brain function in African Americans." *Hum. Brain Mapp.*, vol. 42, no. 6, pp. 1727–1741, (2021), doi: 10.1002/hbm.25324.
- 4- D. J. Kim *et al.*, "Aberrant structural–functional coupling in adult cannabis users." *Hum. Brain Mapp.*, vol. 40, no. 1, pp. 252–261, (2019), doi: 10.1002/hbm.24369.
- 5- P. Manza, E. Shokri-Kojori, and N. D. Volkow, "Reduced Segregation between Cognitive and Emotional Processes in Cannabis Dependence." *Cereb. Cortex*, vol. 30, no. 2, pp. 628–639, (2020), doi: 10.1093/cercor/bhz113.
- 6- M. F. Glasser *et al.*, "A multi-modal parcellation of human cerebral cortex." *Nature*, vol. 536, no. 7615, pp. 171–178, (2016), doi: 10.1038/nature18933.
- 7- M. F. Glasser *et al.*, "SC a Department." *Neuroimage*, (2013), doi: 10.1016/j.neuroimage.2013.04.127.
- 8- M. P. Van Den Heuvel and O. Sporns, "Rich-Club Organization of the Human Connectome." vol. 31, no. 44, pp. 15775–15786, (2011), doi: 10.1523/JNEUROSCI.3539-11.2011.



The Combination of Transcranial Magnetic Stimulation, HRV Biofeedback and Exposure Prevention Response for Resistant Obsessive Compulsive Disorder: An Intensive Day Care Program

Sanaz Khomami* , Roshanak Khodabakhsh Pirklani

Department of Psychology, Faculty of Education and Psychology Alzahra University, Tehran, Iran

*Corresponding Author: Sanaz Khomami
Email: s.khomami@alzahra.ac.ir

Abstract

Obsessive Compulsive Disorder (OCD) is a mental and behavioral disorder in which an individual has intrusive thoughts and rituals which decreases the distress. It seems that there are many treatments such as EX/RP, rTMS, medications or mindfulness for OCD, but there is no single effective treatment yet. In this study we investigated the efficacy of day care rTMS over the Supplementary Motor Area (SMA) with combination of exposure response prevention and biofeedback. In a quasi-experimental design 13 patients were included to the study and received daily rTMS with EX/RP and biofeedback. We utilized BDI, BAI, and YBOCS tools to collect data before and after the treatment and in the subsequent one-month follow-up. According to the BDI, BAI and YBOCS results, the decrease of the score was found to be statistically significant at the $p < 0.001$ level after and one month follow up. The results indicated that the combination of sequenced neuromodulation treatments simultaneously such as rTMS and biofeedback with exposure therapy can facilitate the engagement and enhancement of self-control and distress tolerance.

Keywords: Obsessive Compulsive Disorder; Exposure Prevention Response; Repetitive Transcranial Magnetic Stimulation; Biofeedback.

1. Introduction

Unwanted, repetitive, and distressing thoughts, images, or impulses (obsessions) and time-consuming behaviors (compulsions) with 2-3% lifetime prevalence are the main characteristics of Obsessive Compulsive Disorder (OCD) [1]. The currently approved treatments of OCD are Exposure Response Prevention (ERP) therapy [2], selective serotonin reuptake inhibitors [3], repetitive Transcranial Magnetic Stimulation (rTMS) [4], and intensive residential program [5]. Based on current knowledge the accurate pathophysiology of OCD is not completely clear, but it is supposed that OCD is associated with dysfunctional networks which is due to the orbitofronto-striato-pallido-thalamic circuitry. In addition to the aforementioned traditional psychological and pharmacological treatments, the novel and efficient neuromodulation techniques such as rTMS can be utilized to target the various parts of this circuitry more focally and effectively [6]. Also, the researches indicated that changing sensory experience by mindfulness methods which can be associated with some areas like thalamus can have an impressive effects on response control and subsequently relapse management [7]. Hence, the combination of sequenced neuromodulation treatments such as rTMS and biofeedback with exposure therapy can facilitate the engagement and enhancement of self-control and toleration the distress caused by the response prevention. In this paper, we hypothesized the effect of inhibitory rTMS on SMA and illustrate it can decrease the response inhibition and processing error. We will finally conclude whether this combinatory method tends to be highly efficacious and can significantly enhance compliance with exposure response prevention.

2. Materials and Methods

In one-time series quasi experimental design, 13 patients (10 females and 3 males) between 20 to 50 years of age who were referred to Atieh Clinic after diagnosing with OCD by a psychiatrist according to the fifth version of the American Psychiatric Association Diagnostic and Statistical Manual (DSM5) after completion of a consent form were included to the study. rTMS was administrated at 120% of YBOCS, BDI, and BAI depression tests were completed immediately after 20 sessions and 4 weeks later.

3. Results

13 subjects were included in this study. The mean age of the group was 35 y (± 8 y). Since the inclusion was based on the patients that came for treatment to the clinic with resistance to medications and rTMS inclusion criteria, more females than males were included. As can be seen in the table, the treatment reduced YBOCS total scores from (31.00 ± 3 sdt) to (13 ± 2.00 sdt) at the end of the follow-up which corresponds to a reduction of 18 points. Through repeated measures ANOVA the overall change was significant at $p < 0.0001$ level ($F = 65/09$, $\eta^2 = 0.79$).

4. Conclusion

In this case series study, we proposed a day care program including rTMS with Ex/PR and HRV biofeedback and examined its efficacy in 12 pharmaco-resistant OCD outpatients. There were three novel findings of this study. The first a rapid and significant reduction of symptoms was achieved after just one week of our proposed intensive program, much faster than what was previously seen by utilizing standard weekly CBT (Ex/RP) or pharmacotherapy or rTMS [8-10]. The effectiveness of intensive and daily CBT using Exposure and Response Prevention (ERP) for OCD is well constructed, and it is considered as one of the standard and first-line treatments for OCD [11]. Intensive CBT and "therapy hour" produce improvement in 60-80% of OCD patients in as short as 4 weeks [12]. Another interesting achievement of this study was the increasing patients tolerance and reduction of distress by three factors simultaneously; rTMS, HRV biofeedback, and Ex/RP. As results shows, there was a significant reduction in anxiety scales of 12 patients. Lower Distress Tolerance (DT) is significantly associated with obsessions in nonclinical samples, poorer DT prospectively predicts the frequency of obsessions [13] and is associated with greater anxiety following an experimental task designed to elicit an OCD-like intrusion. On the other hand, HRV is mediated by a complex interplay of the CNS and ANS subsystems, reflecting physiological functioning in a range of psychiatric disorders [14], with implications in emotion regulation and self-awareness [15]. The third, we followed the patients up one month after exposure therapy. The results showed the significance of therapeutic effects among patients. According to the studies, the pathogenesis of OCD is different and involved a network of different areas of the brain. Hence, the best treatment would be to


involve both the subcortical areas (bottom-up pathways) and the cortical areas (top-down pathways). rTMS adhere to exposure and maintain these effects with mindfulness-based biofeedback which has been found to have a significant impact on the treatment of OCD patients. Therefore, additional research is warranted to determine whether these adherences lead to greater symptom improvement.

References

- 1- Michael H Bloch, Angeli Landeros-Weisenberger, Maria C Rosario, Christopher Pittenger, and James F Leckman, "Meta-analysis of the symptom structure of obsessive-compulsive disorder." *American Journal of Psychiatry*, Vol. 165 (No. 12), pp. 1532-42, (2008).
- 2- Rachel Middleton, Michael G Wheaton, Reilly Kayser, and H Blair Simpson, "Treatment resistance in obsessive-compulsive disorder." *Treatment resistance in psychiatry*, pp. 165-77, (2019).
- 3- Minah Kim, Wi Hoon Jung, Geumsook Shim, and Jun Soo Kwon, "The effects of selective serotonin reuptake inhibitors on brain functional networks during goal-directed planning in obsessive-compulsive disorder." *Scientific reports*, Vol. 10 (No. 1), pp. 1-8, (2020).
- 4- Gianluca Serafini *et al.*, "The effects of repetitive transcranial magnetic stimulation on cognitive performance in treatment-resistant depression. A systematic review." *Neuropsychobiology*, Vol. 71 (No. 3), pp. 125-39, (2015).
- 5- Marlene Taube-Schiff, Neil A Rector, Persephone Larkin, Adrienne Mehak, and Margaret A Richter, "Effectiveness of intensive treatment services for obsessive compulsive disorder: outcomes from the first Canadian residential treatment program." *International journal of psychiatry in clinical practice*, Vol. 24 (No. 1), pp. 59-67, (2020).
- 6- Simone Rehn, Guy D Eslick, and Vlasios Brakoulias, "A meta-analysis of the effectiveness of different cortical targets used in repetitive transcranial magnetic stimulation (rTMS) for the treatment of obsessive-compulsive disorder (OCD)." *Psychiatric Quarterly*, Vol. 89 (No. 3), pp. 645-65, (2018).
- 7- Steven I Rudoy, "Developing a model for understanding mindfulness as a potential intervention for obsessive-compulsive disorder." *Pepperdine University*, (2014).
- 8- Parth Dutta *et al.*, "Efficacy of intensive orbitofrontal continuous Theta Burst Stimulation (iOfcTBS) in Obsessive Compulsive Disorder: A Randomized Placebo Controlled Study." *Psychiatry Research*, Vol. 298p. 113784, (2021).
- 9- Madhuri H Nanjundaswamy, Shyam Sundar Arumugham, Janardhanan C Narayanaswamy, and YC Janardhan Reddy, "A prospective study of intensive in-patient treatment for obsessive-compulsive disorder." *Psychiatry Research*, Vol. 291p. 113303, (2020).
- 10- Joseph O'Neill *et al.*, "Effects of intensive cognitive-behavioral therapy on cingulate neurochemistry in obsessive-compulsive disorder." *Journal of psychiatric research*, Vol. 47 (No. 4), pp. 494-504, (2013).
- 11- Hjalti Jónsson, Maria Kristensen, and Mikkel Arendt, "Intensive cognitive behavioural therapy for obsessive-compulsive disorder: a systematic review and meta-analysis." *Journal of Obsessive-Compulsive and related disorders*, Vol. 6pp. 83-96, (2015).
- 12- Victoria B Oldfield, Paul M Salkovskis, and Tracey Taylor, "Time-intensive cognitive behaviour therapy for obsessive-compulsive disorder: A case series and matched comparison group." *British Journal of Clinical Psychology*, Vol. 50 (No. 1), pp. 7-18, (2011).
- 13- Jesse R Cogle, Kiara R Timpano, Kristin E Fitch, and Kirsten A Hawkins, "Distress tolerance and obsessions: an integrative analysis." *Depression and anxiety*, Vol. 28 (No. 10), pp. 906-14, (2011).
- 14- Tao Yang *et al.*, "Abnormal regional homogeneity of drug-naïve obsessive-compulsive patients." *Neuroreport*, Vol. 21 (No. 11), pp. 786-90, (2010).
- 15- Stephen W Porges, "The polyvagal theory: phylogenetic substrates of a social nervous system." *International journal of psychophysiology*, Vol. 42 (No. 2), pp. 123-46, (2001).



Correlation of Brain Oscillation with Executive Function Performance

Mohammad Asadi ¹, Pegah Ramezani ^{2*} 

¹ *Institute for Cognitive Science Studies, Tehran, Iran*

² *University of Tabriz, Tabriz, Iran*

*Corresponding Author: Pegah Ramezani
Email: Pegah.ramezani7504@gmail.com

Abstract

In this study we have recorded EEG signal from 38 people in resting state condition along with some tasks to assess their Executive Function performance. The correlation between Executive Function performance and absolute power of brain signal have demonstrated negative correlation in right frontal in all bands, especially in high Gamma, positive correlation in right and left occipital in Alpha band, positive correlation in central in high Beta band positive correlation in left frontal and left parietal in Theta.

Keywords: Executive Function; Electroencephalography; Cognitive Function; Brain Activity.

1. Introduction

Executive Function (EF) is one of the most complex cognitive functions and having a good EF ability requires coordination between other cognitive functions. Attention, Decision making, planning, working memory and cognitive flexibility are cognitive functions that play role in EF [1]. Researchers have conducted some studies to assess the relationship between brain signal activity and EF performance which is an essential step assessing of EF using EEG. One of this studies conducted by Tarullo et al in 2017 have demonstrated a positive correlation with power of brain signal in Gamma band [2]. Another study by Weiss et al in 2018 shows a significant correlation of anticipatory mu rhythm desynchronization with EF performance [3]. Basharpour *et al.* have addressed the relationship of EF performance with frontal region and have concluded that correlation of frontal channels in Alpha, Beta and Theta band has a positive correlation [4] and Soltani and Arabi demonstrated positive relation of Alpha and Beta Activity with EF performance [5].

2. Materials and Methods

38 individuals (12 female, 26 male) from 20 to 50 years old without any neurological problems participated in this study. EEG data were recorded by a 21-channel (10-20 system) for three minutes. The EEG signal has been recorded in resting state condition and followed by the Shape Stroop task, Shifting, GO/NO GO task to measure the performance of subjects' EF.

Since recording brain waves by EEG without any noise and artifact is inevitable, the first step in processing brain signals is to eliminate these noises. Firstly we applied a band pass Butterworth filter over 4Hz and down at 49Hz. In the next step, we applied the rASR algorithm which has been proved to be very effective in removing noises in both online and offline conditions, another reason for preferring this algorithm to others is that this algorithm comparing to original ASR which itself is one of the fast methods for removing artifact had one third less computational effort [6].

After preprocessing we divided brain signals to six different frequency band, namely Theta (4-8 Hz), Alpha (8-12 Hz), Beta (12-25 Hz), High-Beta (25-30 Hz), Gamma (30-40 Hz), High-Gamma (40-49 Hz) and calculated absolute power for each frequency band and each channel and then we assessed the correlation between each feature and EF performance using Pearson method.

3. Results

According to Figure 1 all parts, you could see a negative correlation between EF performance and absolute power in Right Frontal in all bands, especially in high gamma, positive correlation in right and left occipital in alpha band, positive correlation in central in high beta band positive correlation in left frontal and left parietal in theta, also positive correlation in pre frontal region in gamma and theta band.

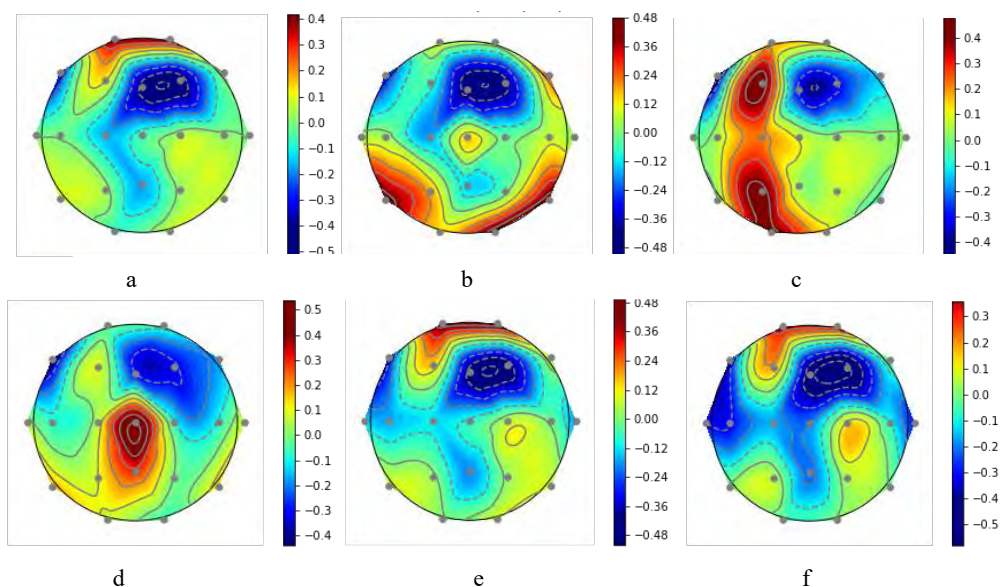


Figure 1. Pearson coefficient of EF performance with Absolute Power in each channel in frequency band (a) Theta (b) Alpha (c) Beta (d) High-Beta (e) Gamma (f) High-Gamma

frontal area [4, 5]. Some studies have shown positive correlation in gamma band but according to our study in gamma band we have both positive and negative correlation but in different areas [2].

Acknowledgment

We wish to acknowledge the help provided by the technical and support staff in the Cambridge Cognition. We would also like to show our deep appreciation to our supervisors who helped me finalize my project.

References

- 1- D. T. Stuss and M. P. Alexander, "Is there a dysexecutive syndrome?." *Philos. Trans. R. Soc. B Biol. Sci.*, vol. 362, no. 1481, pp. 901–915, (2007).
- 2- A. R. Tarullo *et al.*, "Gamma power in rural Pakistani children: Links to executive function and verbal ability." *Dev. Cogn. Neurosci.*, vol. 26, no. March, pp. 1–8, (2017).
- 3- S. M. Weiss, A. N. Meltzoff, and P. J. Marshall, "Neural measures of anticipatory bodily attention in children: Relations with executive function." *Dev. Cogn. Neurosci.*, vol. 34, no. May, pp. 148–158, (2018).
- 4- S. Basharpour, F. Heidari, and P. Molavi, "EEG coherence in theta, alpha, and beta bands in frontal regions and executive functions," *Appl. Neuropsychol.*, vol. 28, no. 3, pp. 310–317, (2021).
- 5- S. Soltani Kouhbanani and S. M. Arabi, "Home executive function environment and executive functions in children: The mediating role of brain electrical activity." *Curr. Psychol.*, (2021).
- 6- S. Blum, N. S. J. Jacobsen, M. G. Bleichner, and S. Debener, "A riemannian modification of artifact subspace reconstruction for EEG artifact handling." *Front. Hum. Neurosci.*, vol. 13, no. April, pp. 1–10, (2019).



Subject-to-Subject Transfer Learning Based on Tensor Decomposition for BCI Application

Zahra Sohrabi-Bonab * , Mohammad-Bagher Shamsollahi

Department of Electrical and Electronics Engineering, Sharif University of Technology, Tehran, Iran

*Corresponding Author: Zahra Sohrabi-Bonab
Email: Pinar454@gmail.com

Abstract

Event-Related Potential (ERP) detection and enhancement and its subcomponents separation are one of the long-established problems in EEG signal processing. ERP data is multi-dimensional, with correlated data in some spaces. This study extends the utility of tensor decomposition to explore the underlying property of a multi-subject ERP/EEG dataset. A subject-to-subject transfer framework is developed for detecting ERP based on a model pool from other subjects and a small amount of calibration training data from a new subject. Therefore, it suggests an affordable way of learning the shared structure of classification rules. With a significant decrease in classification time, an acceptable accuracy is obtained.

Keywords: Event-Related Potential; Tensor Decomposition; Sparsity Regularization; Transfer Learning.

1. Introduction

Electroencephalogram (EEG) is the most common non-invasive signal used in Brain-Computer Interface (BCI) systems. Event-Related Potentials (ERP) are time-locked changes of neuronal activity of brain in response to external stimuli. While ERP detection is the core part of some BCI systems, it suffers from low signal to noise ratio. Therefore, building an optimal common pattern recognition model for different subjects, during different sessions and devices is a challenging task. The subject-to-subject transfer of BCI models can be regarded as a scheme of transfer learning as it reuses the existing knowledge to deal with a new domain. Transfer learning techniques originating from the field of machine learning have been adopted to compensate BCI systems for inter-subject and inter-session variability of EEG feature distributions [1].

In recent years many researchers have used tensor decomposition and its variants as a powerful tool for analyzing multi-dimensional signals such as hyper-spectral image processing [2, 3] and EEG signal processing [4]. In this paper an ERP signal is represented as a 3-order tensor with three factors: channel, time, and trials. The motivation behind using such a method is that the data is correlated in some space. Therefore, multilinear analysis can be carried out based on these tensor spaces. In ERP signal processing, the constructed tensor data often displays a low-rank structure due to significant correlations between neighboring electrodes and similar trials. Therefore, data variation and information are representable with small number of latent factors.

One of the main challenges of BCI systems' development and application is intra/inter-subject variability. This variability comes from changes in neural processing, non-stationarity of EEG and numerous neurophysiological mechanisms [5]. To deal with this challenge, in this work, subject-to-Subject Transfer Learning (STL) framework is developed to detect ERP signal from similar or relevant subjects to facilitate recognition process for a new subject. Basically, STL needs a small amount of training data from a new subject. The proposed framework remarkably reduced the required training time for a new subject.

The work is based on the hypothesis that the similarity of brain dynamics in event-related potential paradigms among individuals is predictable. In order to validate the efficiency of STL model, an experiment on real data is performed. The

results suggest a practical way toward online ERP detection and can set a light to numerous real-world BCI applications.

2. Materials and Methods

We model the ERP data as the three-dimensional tensor $\mathcal{Y} = \mathcal{X} + \mathcal{N}$, where $\mathcal{Y} \in \mathbb{R}^{I_1 \times I_2 \times I_3}$ is a tensorized recorded EEG data, with I_1, I_2, I_3 being channel, time and trial dimensionality, respectively. $\mathcal{X} \in \mathbb{R}^{I_1 \times I_2 \times I_3}$ is a low-rank tensor and superposition of ERP components. Moreover, $\mathcal{N} \in \mathbb{R}^{I_1 \times I_2 \times I_3}$ corresponds to the background EEG and additive noises. In order to separate the low-rank tensor from the noisy one, a regularization term has to be adopted. Therefore, an estimate of \mathcal{X} can be found by minimizing the following cost function, which is composed of a data fidelity term and a regularization term (Equation 1):

$$\begin{aligned} \underset{\mathcal{G}, A_1, A_2, A_3}{\text{argmin}} \quad & \|\mathcal{Y} - \mathcal{X}\|_F^2 + \lambda \|\mathcal{G}\|_1 \\ \text{s. t.} \quad & \mathcal{X} = \mathcal{G} \times_1 A_1 \times_2 A_2 \times_3 A_3 \\ & A_i^T A_i = I, \quad i = 1, 2, 3 \end{aligned} \quad (1)$$

Estimation of multiple unknowns simultaneously and directly is hard. Therefore, ADMM method [3] is adopted to solve objective function of Equation 1. At each iteration of ADMM, we solve the objective function according to one of the constraints while other constraints are considered fixed. Therefore, the core tensor $\mathcal{G} \in \mathbb{R}^{J_1 \times J_2 \times J_3}$ and the factor matrices $A_i \in \mathbb{R}^{J_i \times I_i}$, with $J_i < I_i$, are updated alternatively.

3. Results

The efficiency of the proposed STL algorithm is examined by classification performance. In experiment setup, one subject was successively chosen as the test subject and all other subjects were then used for training. For feature extraction, recorded EEG data from k th subject with N_k trials, $\mathcal{Y}^k \in \mathbb{R}^{I_1 \times I_2 \times N_k}$ was first preprocessed and then it is decomposed with low-rankness and sparsity constraint using Equation 1. For every new test subject s , the feature extraction rule is (Equation 2, 3):

$$f_{train} = \mathcal{Y}_{train}^{(s)} \times_1 A_1^{(k)T} \times_2 A_2^{(k)T} \quad (2)$$

$$f_{test} = \mathcal{Y}_{test}^{(s)} \times_1 A_1^{(k)T} \times_2 A_2^{(k)T} \quad (3)$$

Where, the matrices $A_1^{(k)T}$ and $A_2^{(k)T}$ are transposed factor matrices of the train subject k , f_{train} and f_{test} are train and test feature space, respectively. Test subject specific training data of about one session is given to the algorithm to adapt the bias of the classifier, and the remaining data is used for testing. The feature extraction rule is subsequently applied to the test set, followed by a linear LDA classifier. The dataset from [6] is used for our experiment. More detail about the data and its preprocessing method is available in the original paper [6]. Figure 1 demonstrates the results obtained from STL framework for both 5 blocks and 10 blocks trial repetition. It illustrates the feasibility of subject-to-subject model transferring for ERP detection, and elucidate the performance of the proposed framework with respect to accuracy. The required training time on the average is reduced by 300%.

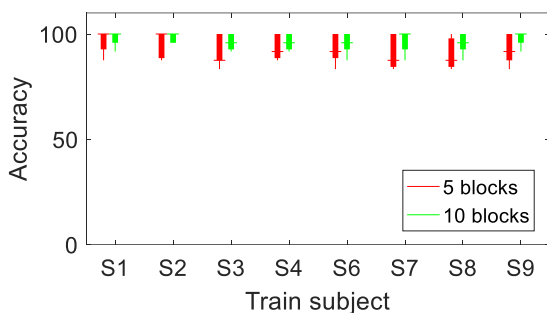


Figure 1. Results obtained from STL framework for both 5 blocks and 10 blocks trial repetition

4. Conclusion

STL model is effective at learning structure between both multiple subjects and multiple sessions in EEG-based BCI tasks. By assuming that the weights of the channels and the features are independent we are able to reduce the size of the feature space by low-rank tensor decomposition. In addition, we also show that STL is useful in the task of subject-to subject transfer where the prediction for an unseen subject is performed based on a model learned from other subjects in the same group.

References

1- Saha, Simanto, and Mathias Baumert. "Intra-and inter-subject variability in EEG-based sensorimotor brain

computer interface: a review.", *Frontiers in computational neuroscience*, 87, (2020).

2- X. Gong, W. Chen, and J. Chen, "A low-rank tensor dictionary learning method for hyperspectral image denoising." *IEEE Transactions on Signal Processing*, vol. 68, pp. 1168–1180, (2020).

3- Y. Chang, L. Yan, X.-L. Zhao, H. Fang, Z. Zhang, and S. Zhong, "Weighted low-rank tensor recovery for hyperspectral image restoration." *IEEE Transactions on Cybernetics*, vol. 50, no. 11, pp. 4558–4572, (2020).

4- M. J. Idaji, M. B. Shamsollahi, and S. H. Sardouie, "Higher order spectral regression discriminant analysis (HOSRDA): A tensor feature reduction method for ERP detection." *Pattern Recognition*, vol. 70, pp. 152–162, (2017).

5- Wei, Chun-Shu, et al. "A subject-transfer framework for obviating inter-and intra-subject variability in EEG-based drowsiness detection.", *NeuroImage*, 174: 407-419, (2018).

6- U. Hoffmann, J.-M. Vesin, T. Ebrahimi, and K. Diserens, "An efficient p300-based brain computer interface for disabled subjects." *Journal of Neuroscience Methods*, vol. 167, no. 1, pp. 115– 125, (2008).



Perceptual Decision Confidence Recognition during Random Dot Kinematogram Task Using EEG and Deep Learning

Alireza Ettefagh, Farnaz Ghasemi * , Zahra Tabanfar

Department of Biomedical Engineering, Amirkabir University of Technology, Tehran, Iran

*Corresponding Author: Farnaz Ghasemi

Email: ghassemi@aut.ac.ir

Abstract

As defined in the encyclopedia of computational neuroscience, perceptual decision-making is the process by which sensory information is used to guide behavior toward the external world. This process has a great impact on humans adaptive behavior. In our previous work, we tried to explore the function of the brain during this type of decisions by examining Event-Related Potentials, Event-Related Spectral Perturbations, and Task Engagement Indices. In this study, a deep learning paradigm is used to classify various confidence conditions using single-trial EEG data. This approach resulted in an accuracy of 80.7% for the binary classification of confidence. The result was, however, poor for the 3-group classification. As a consequence, using neural networks seems effective for recognizing low and high confidence classes without the need of handcrafted feature extraction techniques.

Keywords: Perceptual Decision-Making; Electroencephalography; Deep Learning; Convolutional Neural Network.

1. Introduction

The act of choosing one option from a set of alternatives based on sensory information available in a noisy environment is known as perceptual decision-making. The neurophysiological analysis of the brain during these types of decisions is of great interest due to the serious role of this act in human personal and social life. Choice confidence, or an individual's subjective assessment of decision correctness, is an important factor; however, the functions of choice confidence in the brain during decision making seem to be unclear. The aim of this research is to discriminate between different confidence responses using the results from our previous study [1], and a deep Convolutional Neural Network (CNN).

To this end, EEGNet architecture [2] was used for deep learning. Basically, this CNN architecture has been developed to decode brain states in Brain Computer Interface systems. Its performance has already been investigated using several event-related potential datasets such as Sensory-Motor Rhythm (SMR), P300 visual evoked potentials, error-related negativity response (ERN), and Movement-Related Cortical Potentials (MRCP) [2-4]. Furthermore, it has the ability to sum up a few well-known EEG feature extraction methods like optimal spatial filterbank. It can also be trained on a finite amount of data acquired during the training phase, and produce separable features of the decoder [4].

2. Materials and Methods

Single-trial EEG data, which had been secondary pre-processed in the previous work, were used in this study. These data were collected from 24 healthy participants and consisted of two blocks of 160 trials in 64 channels with a final sampling rate of 1000Hz. To ensure that all channels had an equal number of trials, 11 channels were excluded in this stage because some trials were marked as "excluded" in the original dataset [5]; thus, 53 channels were used for the deep learning stage. Based on the findings from the previous work, the data were segmented into 200ms (0-199ms) intervals time-locked to stimulus onset. Each trial was then labeled as low, medium, or high confidence response based on behavioral data from [5]. Afterwards, for each participant, corresponding 200-point length trials from each channel were arranged from pre-frontal down to parieto-occipital channels into a two-dimensional array, resulting 53×200 input matrices to feed the network. Figure

1 represents an instance of input matrices. The data were then randomly split into training and testing sets (85% for training and 15% for testing).

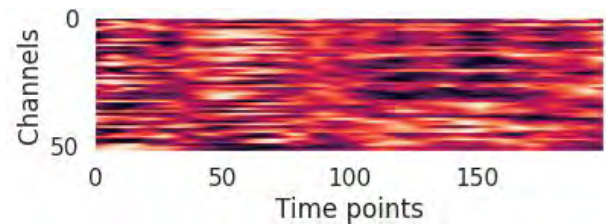


Figure 1. Visualization of an input matrix

3. Results

K-fold cross validation (k=5) was used to evaluate the model. According to the results, the model had a good performance in discriminating between high and low confidence trials. However, the results for high, medium, and low confidence trials were unsatisfactory. Table 1 represents the train and test accuracies for the binary classification.

Table 1. Train and test accuracies for high and low confidence trials

Fold no.	Error	Accuracy
1	0.6097	79.3%
2	0.6779	80.3%
3	0.597	80.41%
4	0.5535	82.03%
5	0.6711	80.99%
Average	0.6218	80.6% ± 0.9%
Test accuracy	-	80.704%

4. Conclusion

In the previous study [1], we discovered that when a user has moderate confidence in his or her response, his or her mental engagement is elevated. Given that the neural network had difficulty classifying this group, it appears that moderate user confidence for AI systems is a challenging class, since excessive user engagement with the task may result in the activation of brain patterns that are not recognizable by the model. According to the results, neural network is an effective tool for recognizing low and high confidence classes without the need for handcrafted feature extraction from the signal.

References

- 1- Alireza Etefagh, Farnaz Ghassemi, and Zahra Tabanfar, "Time-frequency Analysis of Electroencephalogram Signals in a Perceptual Decision-Making Task of Random Dot Kinematograms." *Frontiers in Biomedical Technologies*, Vol. 0 (No. 0), 05/10 (2022).
- 2- Vernon J. Lawhern, Amelia J. Solon, Nicholas R. Waytowich, Stephen M. Gordon, Chou P. Hung, and Brent J. Lance, "EEGNet: a compact convolutional neural network for EEG-based brain-computer interfaces." *Journal of Neural Engineering*, Vol. 15 (No. 5), (2018).
- 3- A. Vahid, M. Muckschel, S. Stober, A. K. Stock, and C. Beste, "Applying deep learning to single-trial EEG data provides evidence for complementary theories on action control." *Commun Biol*, Vol. 3 (No. 1), p. 112, Mar 9 (2020).
- 4- H. Raza, A. Chowdhury, S. Bhattacharyya, and S. Samothrakis, "Single-Trial EEG Classification with EEGNet and Neural Structured Learning for Improving BCI Performance," in *2020 International Joint Conference on Neural Networks (IJCNN)*, 19-24, pp. 1-8 (2020), doi: 10.1109/IJCNN48605.2020.9207100.
- 5- S. P. Gherman, Marios G. "Simultaneous EEG-fMRI - Confidence in perceptual decisions", (2018), doi: 10.18112/OPENNEURO.DS002739.V1.0.0.



High-Level Semantic Representational Similarity between Brain Activity and WordNet during Natural Movie Watching

Yamin Bagheri Davisaraei ^{1*} , Abol Hossein Vahabie ^{2,3,4}

¹ Department of Psychology, Faculty of Psychology and Education, University of Tehran, Tehran, Iran

² School of Electrical and Computer Engineering, College of Engineering, University of Tehran, Tehran, Iran

³ Department of Psychology, Faculty of Psychology and Education, University of Tehran, Tehran, Iran

⁴ School of Cognitive Sciences, Institute for Research in Fundamental Sciences, Tehran, Iran

*Corresponding Author: Yamin Bagheri Davisaraei
Email: yaaminb@gmail.com

Abstract

WordNet is a large lexical database of the English language, which is a set of hierarchical graph-like relationships based on synonymy between words. In this study, we used human connectome project movie-watching functional MRI data, to characterize the similarity of brain representations of high-level semantic categories, to the representation of these categories in WordNet space. We used within-category similarity pattern analysis to find out the relationship between WordNet semantic pattern and brain representation of semantics in ventral and dorsal visual pathways. Our results show, that there is a significant correlation between patterns of activity in some category-selective brain regions, like parahippocampal and fusiform areas in the representation of high order categories and WordNet category representation pattern. but in contrast to classical presumptions, we found a good level of semantic selectivity in the dorsal visual pathway. for example, the intraparietal sulcus in the dorsal pathway shows remarkable selectivity to living categories such as plant. This finding shows there is some sort of graph-like representations in ventral and dorsal visual pathways.

Keywords: Word Net; Ventral Visual Pathway; Dorsal Visual Pathway; Graph; Semantic; Pattern Similarity Analysis.

1. Introduction

The mechanism behind the representation of the outside world in the brain, with millions of different objects, meanings, and categories in order of milliseconds is still an open question in science. Although there are some well-known category-selective areas in the brain, like the Fusiform Face Area (FFA) for faces [1] and the Parahippocampal Place Area (PPA) [2] for locations and buildings, but with the huge variety of meanings and objects of the outside world, it seems impossible for the brain to represent each meaning in a single location on the cortex. The continuous representation model [3], proposes semantic space, as a continuous map that represents smoothly onto the cortical sheet. In this model, neighboring locations of the cortex will represent similar semantic contents. In this study, we used WordNet [4], which is a linguistics model with a large set of directed graphs that represent the relationship between words in synonyms, and hierarchical supra/sub-ordinate relationships, that's called hyperonymy and hyponymy. In this model, each unit or node, or a word can be described as a vector of relationship or adjacency of this unit to other units. we want to extract similarities between this graph-like representation model and brain response. So, we used fMRI time series of natural movie watching tasks from the human connectome project (HCP)(<https://www.humanconnectome.org/study/hcp-young-adult>) dataset. We have chosen person, location, body part, equipment, animal, plant, and food from high order categories of the WordNet model to test our hypothesis about the correlation between adjacency vectors of these categories in the brain and WordNet model. We used ventral and dorsal visual pathways from the multi-modal parcellation atlas [5] to choose adjacent locations on the cortex because these areas show functional similarity and are grouped together in multi-modal tasks of HCP.

2. Materials and Methods

2.1. Dataset and Subjects

We used HCP 7T movies watching task fMRI data for our hypothesis testing. The data was preprocessed with the human connectome project pipeline. Movie

watching task consists of 18 different movie clips with various and rich content of visual stimuli. Data was acquired in four different 15 minutes fMRI sessions. We used 40 random unrelated subjects data, with an age range from 24 to 32 years old, for our study.

2.2. Proposed Method

For each subject, we fitted a stimulus feature matrix, which is based on existence and nonexistence of each stimulus object in each second of the movies to fMRI signal using regularized regression [3]. we calculated the Representational Similarity Matrix (RSM) from all subordinates of seven frequent different high-level categories in stimulus movies. Also we calculated this matrix in our theoretical WordNet graph for the same subordinate categories. We used path similarity indicator which is an index to find the adjacency of two nodes in a graph, based on the shortest path between two nodes. In the following, we calculated Pearson correlation between brain and WordNet RSM for each sub-area of ventral and dorsal visual pathways and high-level categories.

3. Results

First, we have confirmed the plausibility of the graph-like representation of semantic categories in the ventral visual pathway places and faces are two semantic categories that there is selectivity to them in the Parahippocampal Area (PHA) and the Fusiform Complex (FFC). Our proposed model shows there is a significant positive correlation (p -value < 0.001, Bonferroni corrected) between brain pattern and WordNet pattern for location category in PHA but not in FFC. also there is a significant positive correlation (p -value < 0.001, Bonferroni corrected) for the person category between brain pattern and WordNet in the FFC area but not in PHA. This shows some kind of graph-like representation in the brain. Our next step was to find whether there is a graph-like representation in the dorsal visual pathway too. location category was represented in V3a and V6, which is consistent with the dorsal visual pathway as the where pathway. but interestingly we found that IPS significantly represents person, plant, body part, and living objects. Moreover, there are other representations of animals at V7. these results show semantic representation is not limited to the ventral pathway, and the dorsal

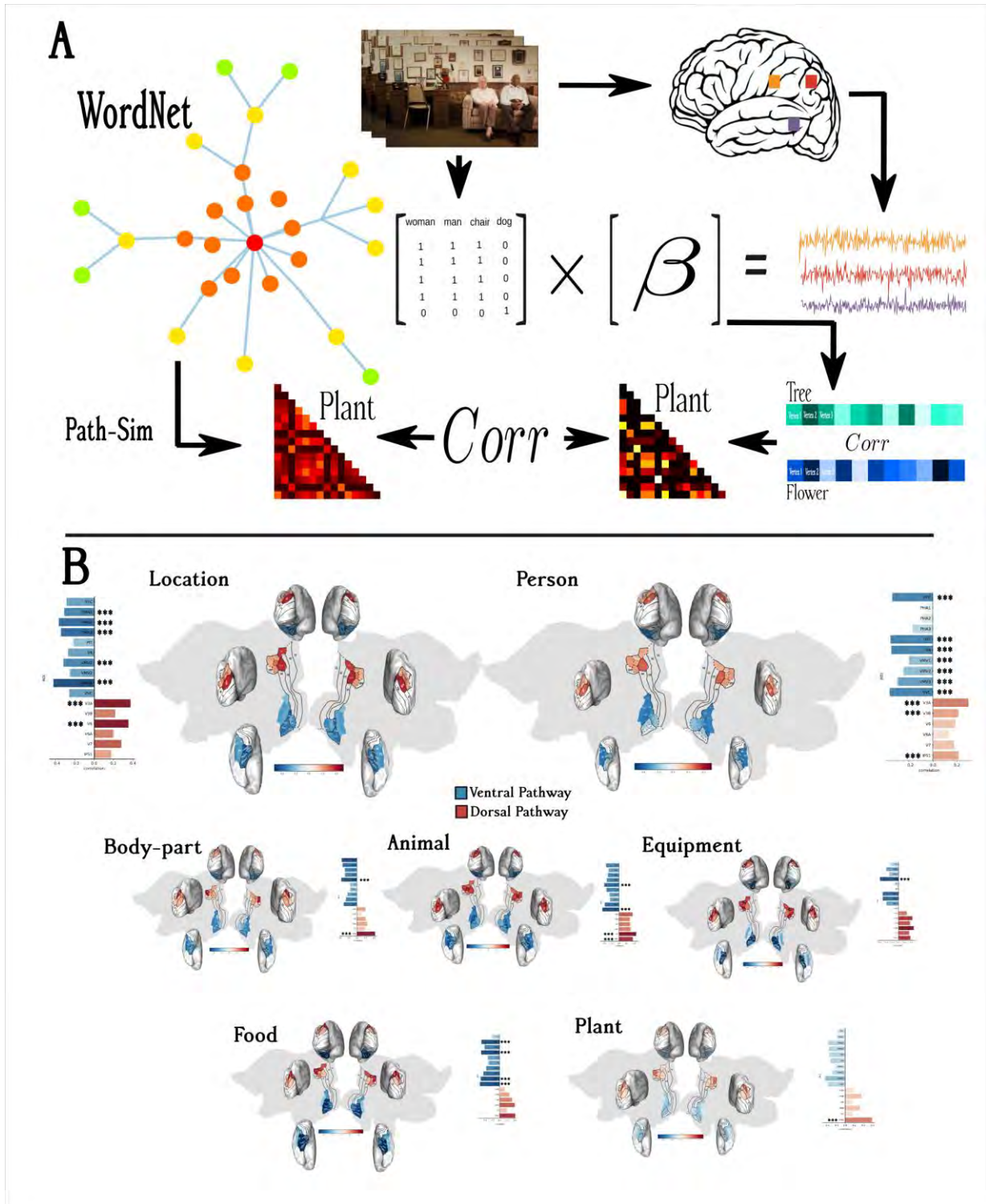


Figure 1. (A) Work flow for experiment and model; (B) Correlation coefficients for brain response and WordNet in the ventral(blue) and dorsal(red) pathways(three stars shows significant correlation with p-value 0.001 and Bonferroni corrected)

visual pathway can not be ignored in the understanding of the brain's semantic representation.

4. Conclusion

Based on our results, there is a positive significant correlation between the representation of some high-level categories in the brain and the WordNet model. This representation is not confined to the ventral visual

pathway and the dorsal pathway importantly represents animals, living things, and also location-related categories. In future studies, we should dig up evolutionary justifications to have such representations in the dorsal visual pathway.

References

- 1- Kanwisher, N., McDermott, J., and Chun, M.M. "The fusiform face area: a module in human extrastriate cortex specialized for face perception.", *J. Neurosci.* 17, 4302–4311, (1997).
- 2- Aguirre, G.K., Zarahn, E., and D'Esposito, M. "An area within human ventral cortex sensitive to "building" stimuli: evidence and implications." *Neuron* 21, 373–383, (1998).
- 3- Huth, A. G., Nishimoto, S., Vu, A. T. & Gallant, J. L. "A continuous semantic space describes the representation of thousands of object and action categories across the human brain.", *Neuron* 76, 1210–1224, (2012).
- 4- Miller, G.A. "WordNet: a lexical database for English." *Commun. ACM* 38, 39–41, (1995).
- 5- Glasser, M. F., Coalson, T. S., Robinson, E. C., Hacker, C. D., Harwell, J., Yacoub, E., ... & Van Essen, D. "CA multi-modal parcellation of human cerebral cortex." *Nature*, 536(7615), 171-178, (2016).



Investigation Capability of Electroencephalography-Based Non-Linear Features in Depression Detection

Mehdi Dehghani* , Majid Torabi, Vahid Asayesh, Sepideh Akhtari Khosroshahi

NPCindex Research Company, Tabriz, Iran

*Corresponding Author: Mehdi Dehghani
Email: dehghanimd@yahoo.com

Abstract

Considering the fact that depression causes a burden on public health and has some adverse effects on depressive patients, the development of a reliable and efficient method for depression diagnosis has high importance. This paper proposed using Electroencephalography (EEG) based on non-linear features and the ability of machine learning algorithms to accurate depression diagnoses. For this aim, Lempel-Ziv Complexity (LZC), Katz Fractal Dimension (KFD), sum of logarithmic (SL) and second-order spectral moment (2M) of the amplitudes of diagonal elements, and normalized entropy (En) of bispectrum in beta and gamma frequency bands in Eyes Closed (EC) and eyes open (EO) condition are examined statistically and classification perspective. The results show that bispectrum SL and 2M features are more statistically significant than other features and the best classification results were obtained using bispectrum 2M in gamma frequency band and temporal brain region with 70% accuracy using a Support Vector Machine (SVM) classifier with Gaussian kernel.

Keywords: Depression Diagnosis; Electroencephalography; Machine Learning; Statistical Analysis; Bispectrum.

1. Introduction

According to the WHO report, more than 300 million people all over the world suffer from depression [1]. Tragic events in life, problems with alcohol or drug consumption, and recently, the Covid 19 pandemic are considered factors leading to depression [2]. Considering the fact that depression causes a burden on public health and has some adverse effects on patients, the development of a reliable and efficient method for depression diagnosis has high importance. Nowadays, the most common way of depression detection is based on clinical interviews. The results of this human-intensive method are dependent on the doctor's experience, therefore besides subjective questionnaires, the brain activity of the patients can be monitored objectively using imaging techniques such as EEG that show mental states, and diseases such as anxiety, psychosis, and depression [3]. Machine learning algorithms have achieved remarkable improvement in the diagnosis of neural disorders. Applications of these methods in depression detection using EEG signals have increased in recent times. Traditionally, EEG power spectrum analysis has been widely used in classifying depressed and normal subjects [4]. Due to the dynamic and nonlinear nature of the EEG signal, it has been proven that non-linear features have more categorizing accuracy than linear features. In the previous studies, the capability of various non-linear features such as KFD and LZC [5-6] was investigated in depression detection. In this study, the performance of bispectrum analysis is evaluated in depression diagnosis and compared with the most used non-linear features (KFD, and LZC) in statistical and classification perspectives.

2. Materials and Methods

First, the EEG signal was recorded from 25 normal (32.72 ± 7.31 years old) and 25 depressed (37 ± 12.50 years old) subjects who were referred to the Asayesh rehabilitation clinic, Tabriz, Iran. In each group 48% of the subjects are female and 52% of them are male.

All of the subjects were medication-free and the diagnosis for them was made by an expert psychiatrist based on DSM-V criteria. The EEG signal was acquired from subjects for 10 minutes (5 minutes in

EC and 5 minutes in EO condition) using Mitsar 19 channel device according to the 10-20 system. After preprocessing recorded signals using low pass, high pass, notch filters, and Infomax Independent Component Analysis (ICA), non-linear features including bispectrum SL, bispectrum 2M, and bispectrum En in beta and gamma frequency bands, KFD, and LZC are extracted from them. Then, the ability of these features in depression detection was investigated using Mann-Whitney statistical test. Also, the classification performance of significant features was evaluated using SVM classifier. In addition to 19 EEG channels, to investigate brain regions' influences on depression detection, the statistical and classification analysis was performed in five brain regions (frontal: Fp1, Fp2, F3, F4, F7, F8, Fz electrodes, central: C3, C4, Cz electrodes, parietal: P3, P4, Pz electrodes, temporal: T3, T4, T5, T6 electrodes and occipital: O1, O2 electrodes) too.

3. Results

The results of the comparison of depressed and healthy groups by Mann-Whitney test ($\alpha \leq 0.01$) have been illustrated in Table 1. According to this table, in EC condition, bispectrum SL, 2M, and KFD are statistically different between two groups, and based on Figure 1, these features are significantly higher in the depressed group. Also according to this figure, temporal and parietal brain regions show the most significant differences. For investigation in detail, the results of region-based analysis also, are illustrated in Table 1. The classification capability of significant features is examined using SVM and 10-fold cross-validation method. Figure 2 shows that temporal bispectrum 2M in gamma frequency band and EO condition achieved the best classification performance with 70% mean accuracy.

4. Conclusion

Findings confirm that bispectral 2M in gamma frequency band and EO condition is a good biomarker for depression detection.

Table 1. Results of the statistical analysis between two groups of depressed and healthy by Mann-Whitney test

Features	EC						EO					
	All	F	C	P	T	O	All	F	C	P	T	O
SL-Beta	0.01	0.20	0.32	0.13	0.26	0.42	0.14	0.69	0.21	0.39	0.22	0.73
SL-Gamma	2.2e-4	0.07	0.09	0.01	0.01	0.23	0.42	0.95	0.93	0.89	0.008	0.99
2M-Beta	0.01	0.20	0.31	0.13	0.26	0.42	0.14	0.69	0.21	0.39	0.22	0.73
2M-Gamma	2.4e-4	0.07	0.10	0.01	0.01	0.23	0.43	0.93	0.95	0.89	0.008	0.99
En-Beta	0.11	0.005	0.20	0.55	0.70	0.51	0.15	0.26	0.40	0.17	0.96	0.10
En-Gamma	0.96	0.55	0.15	0.55	0.13	0.12	0.46	0.62	0.85	0.11	0.81	0.47
KFD	0.01	0.25	0.05	0.22	0.16	0.39	0.03	0.33	0.07	0.55	0.04	0.51
LZC	0.16	0.76	0.32	0.77	0.04	0.75	0.05	0.16	0.66	0.98	0.02	0.95

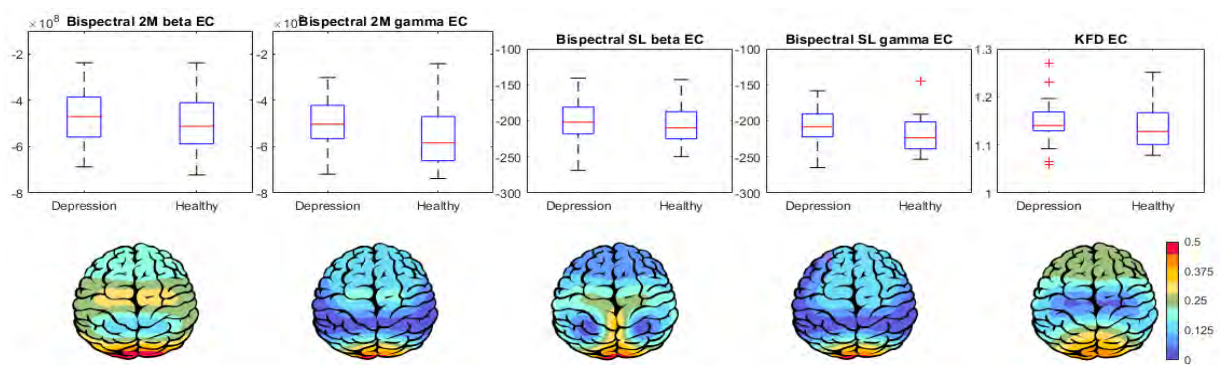


Figure 1. Mean and p-value distribution in the statistically significant features

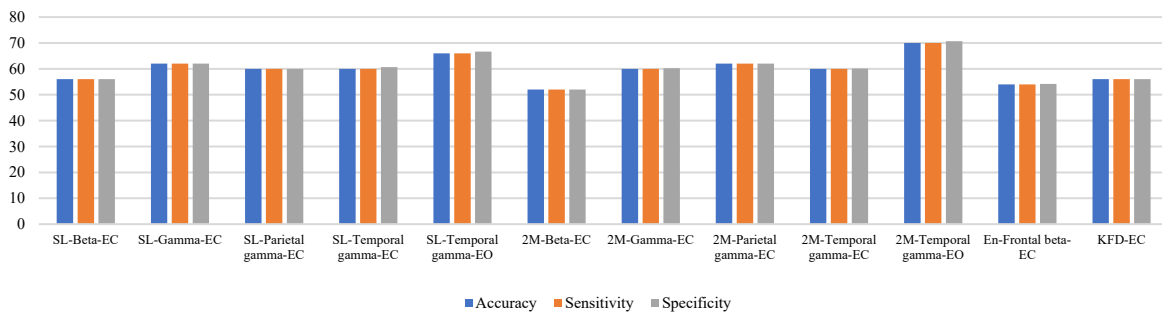


Figure 2. Depressed and healthy groups classification results using SVM

References

- 1- Safayari and H. Bolhasani, "Depression diagnosis by deep learning using EEG signals: A Systematic Review." *Medicine in Novel Technology and Devices*, vol. 12, p. 100102, (2021).
- 2- W. Depression, "Other common mental disorders: global health estimates." *Geneva: World Health Organization*, vol. 24, (2017).
- 3- R. Thibodeau, *et al.*, "Depression, anxiety, and resting frontal EEG asymmetry: a meta-analytic review." *Journal of abnormal psychology*, vol. 115, no. 4, p. 715, (2006).
- 4- W. Mumtaz, *et al.*, "Electroencephalogram (EEG)-based computer-aided technique to diagnose major depressive disorder (MDD)." *Biomedical Signal Processing and Control*, vol. 31, pp. 108-115, (2017).
- 5- M. Bachmann *et al.*, "Methods for classifying depression in single channel EEG using linear and nonlinear signal analysis," *Computer methods and programs in biomedicine*, vol. 155, pp. 11-17, (2018).

- 6- M. Ahmadlou, *et al.*, "Fractality analysis of frontal brain in major depressive disorder." *International Journal of Psychophysiology*, vol. 85, no. 2, pp. 206-211, (2012).



Depression Identification Using Asymmetry Matrix and Machine Learning Algorithms

Majid Torabi Nikjeh* , Mehdi Dehghani, Vahid Asayesh, Sepideh Akhtari Khosroshahi

NPCindex Research Company, Tabriz, Iran

*Corresponding Author: Majid Torabi Nikjeh
Email: torabnikjeh@yahoo.com

Abstract

Developing an efficient and reliable method for the identification of depression has high importance. Electroencephalography (EEG) has shown its potential in this topic. This paper, proposed an approach for depression diagnosis using an interhemispheric asymmetry matrix and machine learning algorithms. The results show that beta absolute power asymmetry in occipital region and eyes open (EC) condition achieve the best depression identification result with 77.1% accuracy using Gaussian Support Vector Machine (SVM) classifier.

Keywords: Depression; Electroencephalogram; Asymmetry Matrix; Machine Learning Algorithms.

1. Introduction

Depression is a major mental disorder and all over the world, approximately 800,000 people die due to it every year [1]. Depression is characterized by loss of interest, lack of motivation, feeling sadness, hopelessness, and even suicidal thoughts. Traditional depression diagnosis depends on subjective evaluation using interview sessions and psychiatric scales. These methods are useful but time-consuming and may lead to misdiagnoses due to environmental and human factors. Therefore, it is crucial to develop an accurate method for classifying depressed and healthy subjects. For this aim, the brain activity of the patients can be monitored objectively using imaging techniques. Among various imaging modalities, EEG has gained attention as it is non-invasive and cost-effective with high temporal resolution [2]. Nowadays, EEG-based depression diagnosis using machine learning algorithms is of great interest. Studies [3] show that interhemispheric frontal alpha asymmetry is a key marker of the human brain in depression detection. Except for alpha frequency band, activities in other brain regions and frequency bands may also be associated with depression. This paper investigates absolute and relative power of theta and beta frequency bands, Individual Alpha peak Frequency (IAF), and theta-to-alpha power ratio features asymmetry capability in depression detection using statistical analysis and machine learning algorithms.

2. Materials and Methods

In this study, EEG signal was acquired from 48 subjects (24 depressed patients and 24 healthy subjects) who were referred to the Asayesh

rehabilitation clinic, Tabriz, Iran. In each group 50% of the subjects are female and 50% of them are male.

All of the subjects were medication-free and the diagnosis for them was made by an expert psychiatrist based on DSM-V criteria. The EEG signal was acquired from subjects for 5 minutes in Eyes Closed (EC) and 5 minutes in EO condition using Mitsar 19 channel device according to the 10-20 system. For reject artifacts, low pass, high pass, and notch filters were used to filter out unnecessary signals. Then, Infomax Independent Component Analysis (ICA) was applied to remove ocular artifacts. After preprocessing data, interhemispheric asymmetry for absolute and relative powers of theta and beta frequency bands, theta-to-alpha power ratio, and IAF features were computed based on Equation 1:

$$A(ch1, ch2) = \frac{F_{ch1} - F_{ch2}}{F_{ch1} + F_{ch2}} \quad (1)$$

Where ch1 is a channel in the left hemisphere and ch2 is the analogous channel of ch1 in the right hemisphere. F_{ch} defines the specific feature value in channel ch. Then, an asymmetry matrix according to Figure 1 is proposed to express the asymmetry values of each feature. This matrix is used as a feature for statistical and classification analysis. In this paper, classification was performed using SVM, logistic regression, and Multi-Layer Perceptron (MLP) algorithms to compare different methods' abilities in depression detection.

3. Results

The results of the comparison of healthy and depressed groups using whole 19 EEG channels and

Table 1. Results of the statistical analysis between two groups of depressed and healthy by Mann-Whitney test

Features	EC						EO					
	All	F	C	P	T	O	All	F	C	P	T	O
Theta absolute power asymmetry	0.43	0.24	0.01	0.65	0.005	0.15	0.26	0.42	0.42	0.26	0.40	0.50
Beta absolute power asymmetry	0.88	0.99	0.28	0.79	0.09	0.08	0.14	0.20	0.54	0.47	0.96	0.01
Theta relative power asymmetry	0.74	0.75	0.58	0.95	0.63	0.70	0.16	0.88	0.17	0.94	0.003	0.38
Beta relative power asymmetry	0.16	0.16	0.30	0.78	0.17	0.46	0.62	0.53	0.94	0.57	0.92	0.48
Theta-to-alpha power ratio asymmetry	0.73	0.61	0.47	0.87	0.35	0.71	0.14	0.19	0.38	0.54	0.0012	0.12
IAF asymmetry	0.29	0.27	0.01	0.55	0.03	0.73	0.78	0.55	0.17	0.94	0.05	0.78

brain regions in EC and EO conditions are illustrated in Table 1. For statistical analysis Mann-Whitney test ($\alpha \leq 0.05$) has been used. According to the results, 19 channel features don't show any significant differences between depressed and healthy groups.

But, in region-based analysis, these features show significant differences between two groups. The mean value and classification accuracy of significant features are illustrated in Figure 2 and Figure 3 respectively.

$A(Fp1,Fp2)$	$A(T3,T4)$
$A(F3,F4)$	$A(T5,T6)$
$A(F7,F8)$	$A(P3,P4)$
$A(C3,C4)$	$A(O1,O2)$

Figure 1. Asymmetry matrix. Orange, yellow, blue, green, and gray cells define frontal, central, temporal, parietal, and occipital regions asymmetry

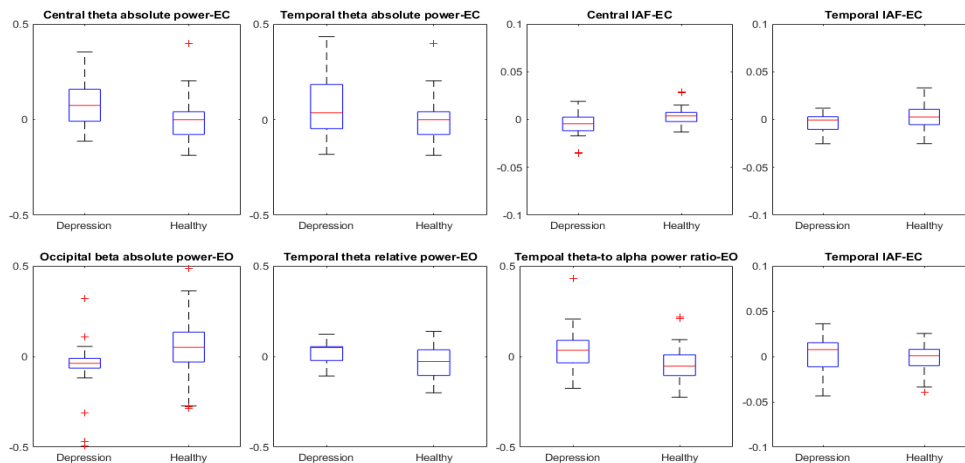


Figure 2. Mean value of significant features in depressed and healthy groups

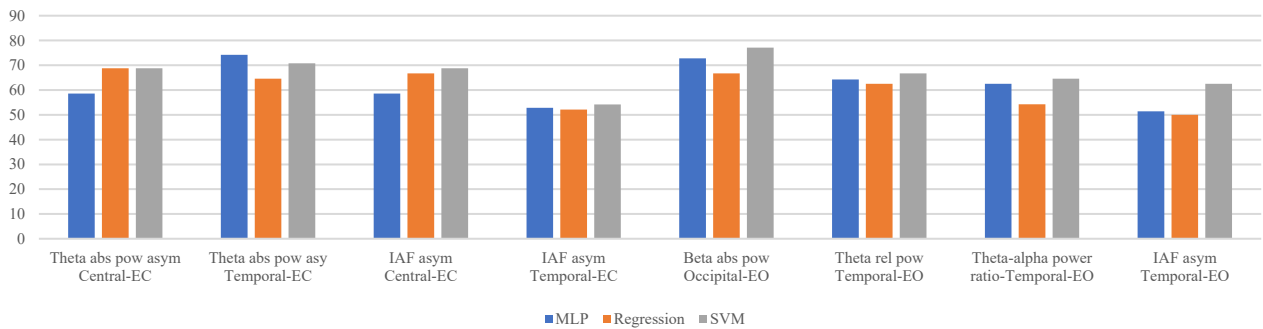


Figure 3. Classification accuracy of healthy and depressed subjects using significant features and SVM, MLP, and regression methods

4. Conclusion

Findings show that beta absolute power asymmetry in occipital region and EO condition is a good biomarker for depression identification with 77.1% accuracy using Gaussian SVM classifier.

References

- 1- H. Cai *et al.*, "A pervasive approach to EEG-based depression detection." *Complexity*, vol. 2018, (2018).
- 2- B. Ay *et al.*, "Automated depression detection using deep representation and sequence learning with EEG signals." *Journal of medical systems*, vol. 43, no. 7, pp. 1-12, (2019).

- 3- W. Mumtaz, *et al.*, "Electroencephalogram (eeg)-based computer-aided technique to diagnose major depressive disorder (mdd)." *Biomed. Signal Process. Control* 31, 108–115, (2017).